Mon. Not. R. Astron. Soc. **000**, 000–000 (0000) Printed 1 February 2008 (MN LATEX style file v2.2)

A binary model for the UV-upturn of elliptical galaxies

Z. Han[1⋆], Ph. Podsiadlowski[2], A.E. Lynas-Gray[2]
[1] *National Astronomical Observatories / Yunnan Observatory, the Chinese Academy of Sciences, Kunming, 650011, China*
[2] *University of Oxford, Department of Physics, Keble Road, Oxford, OX1 3RH*

1 February 2008

ABSTRACT

The discovery of a flux excess in the far-ultraviolet (UV) spectrum of elliptical galaxies was a major surprise in 1969. While it is now clear that this UV excess is caused by an old population of hot helium-burning stars without large hydrogen-rich envelopes, rather than young stars, their origin has remained a mystery. Here we show that these stars most likely lost their envelopes because of binary interactions, similar to the hot subdwarf population in our own Galaxy. We have developed an evolutionary population synthesis model for the far-UV excess of elliptical galaxies based on the binary model developed by Han et al. (2002, 2003) for the formation of hot subdwarfs in our Galaxy. Despite its simplicity, it successfully reproduces most of the properties of elliptical galaxies with a UV excess: the range of observed UV excesses, both in $(1550 - V)$ and $(2000 - V)$, and their evolution with redshift. We also present colour-colour diagrams for use as diagnostic tools in the study of elliptical galaxies. The model has major implications for understanding the evolution of the UV excess and of elliptical galaxies in general. In particular, it implies that the UV excess is not a sign of age, as had been postulated previously, and predicts that it should not be strongly dependent on the metallicity of the population, but exists universally from dwarf ellipticals to giant ellipticals.

Key words: galaxies: elliptical and lenticular, cD – galaxies : starburst – ultraviolet: galaxies – stars: binaries: close – stars: subdwarfs

1 INTRODUCTION

A long-standing problem in the study of elliptical galaxies is the far-ultraviolet (UV) excess in their spectra. Traditionally, elliptical galaxies were supposed to be passively evolving and not contain any young stars that radiate in the far-UV. Therefore, the discovery of an excess of radiation in the far-UV by the *Orbiting Astronomical Observatory* mission 2 (OAO-2) (Code 1969) came as a complete surprise. Indeed, this was one of the first major discoveries in UV astronomy and became a basic property of elliptical galaxies. This far-UV excess is often referred to as the "UV-upturn", since the flux increases in the spectral energy distributions of elliptical galaxies as the wavelength decreases from 2000 to 1200Å. The UV-upturn is also known as UV rising-branch, UV rising flux, or simply UVX (see the review by O'Connell 1999).

The UV-upturn phenomenon exists in virtually all elliptical galaxies and is the most variable photometric feature. A famous correlation between UV-upturn magnitude and metallicity was found by Burstein et al. (1988) from *International Ultraviolet Explorer Satellite* (IUE) spectra of 24 quiescent early-type galaxies (hereafter BBBFL relation). The UV-upturn could be important in many respects: for the formation history and evolutionary properties of stars, the chemical enrichment of galaxies, galaxy dynamics, constraints to the stellar age and metallicity of galaxies and realistic "K-corrections" (O'Connell 1999; Yi, Demarque & Oemler 1998; Brown 2004; Yi 2004). In particular, the UV-upturn has been proposed as a possible age indicator for giant elliptical galaxies (Bressan, Chiosi & Tantalo 1996; Chiosi, Vallenari & Bressan 1997; Yi et al. 1999). The origin of the UV-upturn, however, has remained one of the great mysteries of extragalactic astrophysics for some 30 years (Brown 2004), and numerous speculations have been put forward to explain it: non-thermal radiation from an active galactic nucleus (AGN), young massive stars, the central stars of planetary nebulae (PNe) or post-asymptotic giant branch (PAGB) stars, horizontal branch (HB) stars and post-HB stars (including post-early AGB stars and AGB-manqué stars) and accreting white dwarfs (Code 1969; Hills 1971; Gunn, Stryker & Tinsley 1981; Nesci & Perola 1985; Mochkovitch 1986; Kjærgaard 1987; Greggio & Renzini 1990). Using observations made with the the Hopkins Ultraviolet Telescope (HUT) and comparing them to synthetic spectra, Ferguson et al. (1991) and subsequent studies by Brown, Ferguson & Davidsen (1995), Brown et al. (1997), and Dorman, O'Connell & Rood (1995) were able to show that the UV upturn is mainly caused by extreme horizontal branch (EHB) stars. Brown et al. (2000b) detected EHB stars for the first time in an elliptical galaxy (the core of M 32) and therefore provided direct evidence for the EHB origin of the UV-upturn.

EHB stars, also known as subdwarf B (sdB) stars, are core-helium-burning stars with extremely thin hydrogen envelopes

⋆ E-mail: zhanwenhan@hotmail.com

($M_{\rm env} \leq 0.02 M_{\odot}$), and most of them are believed to have masses around $0.5 M_{\odot}$ (Heber 1986; Saffer et al. 1994), as has recently been confirmed asteroseismologically in the case of PG 0014+067 (Brassard et al. 2001). They have a typical luminosity of a few $L_{\odot}$, a lifetime of $\sim 2 \times 10^8$yr, and a characteristic surface temperature of $\sim 25\ 000$K (Dorman, Rood & O'Connell 1993; D'Cruz et al. 1996; Han et al. 2002). The origin of those hot, blue stars, as the major source of the far UV radiation, has remained an enigma in evolutionary population synthesis (EPS) studies of elliptical galaxies. Two models, both involving single-star evolution, have previously been proposed to explain the UV-upturn: a metal-poor model (Lee 1994; Park & Lee 1997) and a metal-rich model (Bressan, Chiosi & Fagotto 1994; Bressan, Chiosi & Tantalo 1996; Tantalo et al. 1996; Yi et al. 1995; Yi, Demarque & Kim 1997; Yi, Demarque & Oemler 1997; Yi, Demarque & Oemler 1998).

The metal-poor model ascribes the UV-upturn to an old metal-poor population of hot subdwarfs, blue core-helium-burning stars, that originate from the low-metallicity tail of a stellar population with a wide metallicity distribution (Lee 1994; Park & Lee 1997). This model explains the BBBFL relation since elliptical galaxies with high average metallicity tend to be older and therefore have stronger UV-upturns. The model tends to require a very large age of the population (larger than the generally accepted age of the Universe), and it is not clear whether the metal-poor population is sufficiently blue or not. Moreover, the required low-metallicity appears inconsistent with the large metallicity inferred for the majority of stars in elliptical galaxies (Zhou, Véron-Cetty & Véron 1992; Terlevich & Forbes 2002; Thomas et al. 2005).

In the metal-rich model the UV-upturn is caused by metal-rich stars that lose their envelopes near the tip of the first-giant branch (FGB). This model (Bressan, Chiosi & Fagotto 1994; Yi, Demarque & Oemler 1997) assumes a relatively high metallicity – consistent with the metallicity of typical elliptical galaxies ($\sim 1-3$ times the solar metallicity). In the model, the mass-loss rate on the red-giant branch, usually scaled with the Reimer's rate (Reimers 1975), is assumed to be enhanced, where the coefficient $\eta_{\rm R}$ in the Reimer's rate is taken to be $\sim 2-3$ times the canonical value. In order to reproduce the HB morphology of Galactic globular clusters, either a broad distribution of $\eta_{\rm R}$ is postulated (D'Cruz et al. 1996), or, alternatively, a Gaussian mass-loss distribution is applied that is designed to reproduce the distribution of horizontal-branch stars of a given age and metallicity (Yi, Demarque & Oemler 1997). This model also needs a population age that is generally larger than 10 Gyr. To explain the BBBFL UV-upturn – metallicity relation, the Reimer's coefficient $\eta_{\rm R}$ is assumed to increase with metallicity, and the enrichment parameter for the helium abundance associated with the increase in metallicity, $\frac{\Delta Y}{\Delta Z}$, needs to be > 2.5.

Both of these models are quite *ad hoc*: there is neither observational evidence for a very old, low-metallicity sub-population in elliptical galaxies, nor is there a physical explanation for the very high mass loss required for just a small subset of stars. Furthermore, the onset of the formation of the hot subdwarfs is very sudden as the stellar population evolves, and both models require a large age for the production of the hot stars. As a consequence, the models predict that the UV upturn of elliptical galaxies declines rapidly with redshift. However, this does not appear to be consistent with recent observations with the *Hubble Space Telescope* (HST) (Brown et al. 1998; Brown et al. 2000a; Brown et al. 2003). The recent survey with the *Galaxy Evolution Explorer* (GALEX) satellite (Rich et al. 2005) showed that the intrinsic UV-upturn seems not to decrease in strength with redshift.

The BBBFL relation shows that the $(1550-V)$ colour becomes bluer with metallicity (or Lick spectral index $\rm Mg_2$), where $(1550-V)$ is the far-UV magnitude relative to the V magnitude. The relation could support the metal-rich model. However, the correlation is far from being conclusively established. Ohl et al. (1998) studied the far-UV colour gradients in 8 early-type galaxies and found no correlation between the FUV-*B* colour gradients and the internal metallicity gradients based on the $\rm Mg_2$ spectral line index, a result not expected from the BBBFL relation. Deharveng, Boselli & Donas (2002) studied the far-UV radiation of 82 early-type galaxies, a UV-flux selected sample, and compared them to the BBBFL sample, investigating individual objects with a substantial record in the refereed literature spectroscopically[1]. They found no correlation between the $(2000-V)$ colour and the $\rm Mg_2$ spectral index. Rich et al. (2005) also found no correlation in a sample of 172 red quiescent early-type galaxies observed by GALEX and the *Sloan Digital Sky Survey* (SDSS). Indeed, if there is a weak correlation in the data, the correlation is in the opposite sense to that of BBBFL: metal-rich galaxies have redder $(FUV-r)_{\rm AB}$ (far-UV magnitude minus red magnitude). On the other hand, Boselli et al. (2005), using new GALEX data, reported a mild positive correlation between $(FUV-NUV)_{\rm AB}$, which is the far-UV magnitude relative to the near-UV, and metallicity in a sample of early-type galaxies in the Virgo Cluster. Donas et al. (2006) use GALEX photometry to construct colour-colour relationships for nearby early-type galaxies sorted by morphological type. They also found a marginal positive correlation between $(FUV-NUV)_{\rm AB}$ and metallicity. These correlations, however, do not necessarily support the BBBFL relation, as neither Boselli et al. (2005) nor Donas et al. (2006) show that $(FUV-r)_{\rm AB}$ correlates significantly with metallicity. Therefore, this apparent lack of an observed correlation between the strength of the UV-upturn and metallicity casts some doubt on the metal-rich scenario.

Both models ignore the effects of binary evolution. On the other hand, hot subdwarfs have long been studied in our own Galaxy (Heber 1986; Green, Schmidt & Liebert 1986; Downes 1986; Saffer et al. 1994), and it is now well established that the vast majority of (and quite possibly all) Galactic hot subdwarfs are the results of binary interactions. Observationally, more than half of Galactic hot subdwarfs are found in binaries (Ferguson, Green & Liebert 1984; Allard et al. 1994; Thejll, Ulla & MacDonald 1995; Ulla & Thejll 1998; Aznar Cuadrado & Jeffery 2001; Maxted et al. 2001; Williams et al. 2001; Reed & Stiening 2004), and orbital parameters have been determined for a significant sample (Jeffery & Pollacco 1998; Koen, Orosz & Wade 1998; Saffer, Livio & Yungelson 1998; Kilkenny et al. 1999; Moran et al. 1999; Orosz & Wade 1999; Wood & Saffer 1999; Maxted, Marsh & North 2000; Maxted et al. 2000; Maxted et al. 2001; Napiwotzki et al. 2001; Heber et al. 2002; Heber et al. 2004; Morales-Rueda, Maxted & Marsh 2004; Charpinet et al. 2005; Morales-Rueda et al. 2006). There has also been substantial theoretical progress (Mengel, Norris & Gross 1976; Webbink 1984; Iben & Tutukov 1986; Tutukov & Yungelson 1990; D'Cruz et al. 1996; Sweigart 1997). Recently, Han et al. (2002;

[1] Note, however, that some of the galaxies show hints of recent star formation (Deharveng, Boselli & Donas 2002).

2003) proposed a binary model (hereafter HPMM model) for the formation of hot subdwarfs in binaries and single hot subdwarfs. In the model, there are three formation channels for hot subdwarfs, involving common-envelope (Paczyński 1976) ejection for hot subdwarf binaries with short orbital periods, stable Roche lobe overflow for hot subdwarfs with long orbital periods, and the merger of helium white dwarfs to form single hot subdwarfs. The model can explain the main observational characteristics of hot subdwarfs, in particular, their distributions in the orbital period–minimum companion mass diagram and in the effective temperature–surface gravity diagram, their distributions of orbital period and mass function, their binary fraction and the fraction of hot subdwarf binaries with white dwarf (WD) companions, their birth rates and their space density. More recent observations (e.g. Lisker et al. 2004, 2005) support the HPMM model, and the model is now widely used in the study of hot subdwarfs (e.g. Heber et al. 2004, Morales-Rueda, Maxted & Marsh 2004, Charpinet et al. 2005, Morales-Rueda et al. 2006).

Hot subdwarfs radiate in UV, and we can apply the HPMM scenario without any further assumptions to the UV-upturn problem of elliptical galaxies. The only assumption we have to make is that the stellar population in elliptical galaxies, specifically their binary properties, are similar to those in our own galaxy. Indeed, as we will show in this paper, the UV flux from hot subdwarfs produced in binaries is important. This implies that any model for elliptical galaxies that does not include these binary channels is *necessarily* incomplete or has to rely on the *apriori* implausible assumption that the binary population in elliptical galaxies is intrinsically different. The main purpose of this paper is to develop an *apriori* EPS model for the UV-upturn of elliptical galaxies, by employing the HPMM scenario for the formation of hot subdwarfs, and to compare the model results with observations.

The outline of the paper is as follows. We describe the EPS model in Section 2 and the simulations in Section 3. In Section 4 we present the results and discuss them, and end the paper with a summary and conclusions in Section 5.

2 THE MODEL

EPS is a technique for modelling the spectrophotometric properties of a stellar population using our knowledge of stellar evolution. The technique was first devised by Tinsley (Tinsley 1968) and has experienced rapid development ever since (Bruzual & Charlot 1993; Worthey 1994; Bressan, Chiosi & Fagotto 1994; Tantalo et al. 1996; Zhang et al. 2002; Bruzual & Charlot 2003; Zhang et al. 2004a). Recently, binary interactions have also been incorporated into EPS studies (Zhang et al. 2004b; Zhang et al. 2005a; Zhang, Li & Han 2005b; Zhang & Li 2006) with the rapid binary-evolution code developed by Hurley, Tout & Pols (2002). In the present paper we incorporate the HPMM model into EPS by adopting the binary population synthesis (BPS) code of Han et al. (2003), which was designed to investigate the formation of many interesting binary-related objects, including hot subdwarfs.

2.1 The BPS code and the formation of hot subdwarfs

The BPS code of Han et al. was originally developed in 1994 and has been updated regularly ever since (Han, Podsiadlowski & Eggleton 1994; Han 1995; Han, Podsiadlowski & Eggleton 1995; Han et al. 1995; Han 1998; Han et al. 2002; Han et al. 2003; Han & Podsiadlowski 2004). With the code, millions of stars (including binaries) can be evolved simultaneously from the zero-age main sequence (ZAMS) to the white-dwarf (WD) stage or a supernova explosion. The code can simulate in a Monte-Carlo way the formation of many types of stellar objects, such as Type Ia supernovae (SNe Ia), double degenerates (DDs), cataclysmic variables (CVs), barium stars, planetary nebulae (PNe) and hot subdwarfs. Note that "hot subdwarfs" in this paper is used as a collective term for subdwarf B stars, subdwarf O stars, and subdwarf OB stars. They are core-helium-burning stars with thin hydrogen envelopes and radiate mainly in the UV (see Figure 1 for the formation channels of hot subdwarfs).

The main input into the BPS code is a grid of stellar models. For the purpose of this paper, we use a Population I (pop I) grid with a typical metallicity $Z = 0.02$. The grid, calculated with Eggleton's stellar evolution code (Eggleton 1971; Eggleton 1972; Eggleton 1973; Han, Podsiadlowski & Eggleton 1994; Pols et al. 1995; Pols et al. 1998), covers the evolution of normal stars in the range of $0.08 - 126.0 M_{\odot}$ with hydrogen abundance $X = 0.70$ and helium abundance $Y = 0.28$, helium stars in the range of $0.32 - 8.0 M_{\odot}$ and hot subdwarfs in the range of $0.35 - 0.75 M_{\odot}$ (see Han et al. 2002, 2003 for details). Single stars are evolved via interpolations in the model grid. In this paper, we use $t_{\rm FGB}$ instead of $\log m$ as the interpolation variable between stellar evolution tracks, where $t_{\rm FGB}$ is the time from the ZAMS to the tip of the FGB for a given stellar mass m and is calculated from fitting formulae. This is to avoid artefacts in following the time evolution of hot subdwarfs produced from a stellar population.

The code needs to model the evolution of binary stars as well as of single stars. The evolution of binaries is more complicated due to the occurrence of Roche lobe overflow (RLOF). The binaries of main interest here usually experience two phases of RLOF: the first when the primary fills its Roche lobe which may produce a WD binary, and the second when the secondary fills its Roche lobe.

The mass gainer in the first RLOF phase is most likely a main-sequence (MS) star. If the mass ratio $q = M_1/M_2$ at the onset of RLOF is lower than a critical value, $q_{\rm crit}$, RLOF is stable (Paczyński 1965; Paczyński, Ziółkowski & Żytkow 1969; Plavec, Ulrich & Polidan 1973; Hjellming & Webbink 1987; Webbink 1988; Soberman, Phinney & van den Heuvel 1997; Han et al. 2001). For systems experiencing their first phase of RLOF in the Hertzsprung gap, we use $q_{\rm crit} = 3.2$ as is supported by detailed binary-evolution calculations of Han et al. (2000). For the first RLOF phase on the FGB or asymptotic giant branch (AGB), we mainly use $q_{\rm crit} = 1.5$. Full binary calculations (Han et al. 2002) demonstrate that $q_{\rm crit} \sim 1.2$ is typical for RLOF in FGB stars. We do not explicitly include tidally enhanced stellar winds (Tout & Eggleton 1988; Eggleton & Tout 1989; Han et al. 1995) in our calculation. Using a larger value for $q_{\rm crit}$ is equivalent to including a tidally enhanced stellar wind to some degree while keeping the simulation simple (see HPMM for details). Alternatively, we also adopt $q_{\rm crit} = 1.2$ in order to examine the consequences of varying this important criterion.

For stable RLOF, we assume that a fraction $\alpha_{\rm RLOF}$ of the mass lost from the primary is transferred onto the gainer, while the rest is lost from the system ($\alpha_{\rm RLOF} = 1$ means that RLOF is conservative). Note, however, that we assume that mass transfer is always conservative when the donor is a MS star. The mass lost from the system also takes away a specific angular momentum α in units of the specific angular momentum of the system. The unit is expressed as $2\pi a^2/P$, where a is the separation and P is the orbital period of the binary (see Podsiadlowski, Joss & Hsu 1992 for

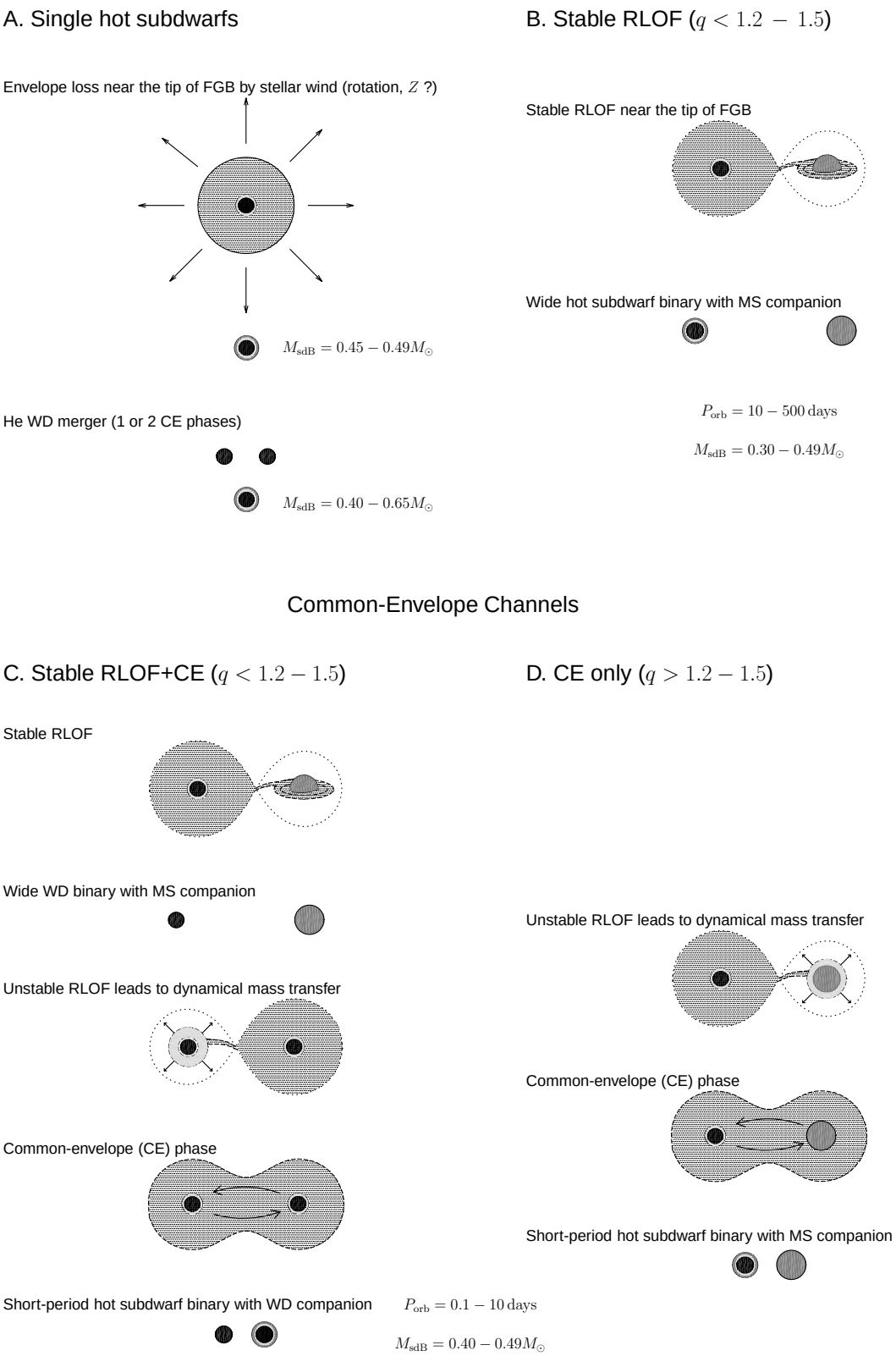

Figure 1. Single and binary channels to produce hot subdwarfs, core-helium-burning stars with no or small hydrogen-rich envelopes. **(A)** Single hot subdwarfs may result from large mass loss near the tip of the first giant branch (FGB), as in the metal-rich model, or from the merger of two helium white dwarfs. **(B)** Stable Roche lobe overflow (RLOF) near the tip of the FGB produces hot subdwarfs in wide binaries. **(C + D)** Common-envelope evolution leads to hot subdwarfs in very close binaries, where the companion can either be a white dwarf (C) or a main-sequence star (D). The simulations presented in this paper include all channels except for the metal-rich single star channel.

details). Stable RLOF usually results in a wide WD binary. Some of the wide WD binaries may contain hot subdwarf stars and MS companions if RLOF occurs near the tip of the FGB (*1st stable RLOF channel* for the formation of hot subdwarfs). In order to reproduce Galactic hot subdwarfs, we use $\alpha_{\rm RLOF} = 0.5$ and $\alpha = 1$ for the first stable RLOF in all systems except for those on the MS (see HPMM for details).

If RLOF is dynamically unstable, a common envelope (CE) may be formed (Paczyński 1976), and if the orbital energy deposited in the envelope can overcome its binding energy, the CE may be ejected. For the CE ejection criterion, we introduced two model parameters, $\alpha_{\rm CE}$ for the common envelope ejection efficiency and $\alpha_{\rm th}$ for the thermal contribution to the binding energy of the envelope, which we write as

$$\alpha_{\rm CE}\,\Delta E_{\rm orb} > E_{\rm gr} - \alpha_{\rm th}\,E_{\rm th}, \qquad (1)$$

where $\Delta E_{\rm orb}$ is the orbital energy that is released, $E_{\rm gr}$ is the gravitational binding energy and $E_{\rm th}$ is the thermal energy of the envelope. Both $E_{\rm gr}$ and $E_{\rm th}$ are obtained from full stellar structure calculations (see Han, Podsiadlowski & Eggleton 1994 for details; also see Dewi & Tauris 2000) instead of analytical approximations. CE ejection leads to the formation of a close WD binary. Some of the close WD binaries may contain hot subdwarf stars and MS companions if the CE occurs near the tip of the FGB (*1st CE channel* for the formation of hot subdwarfs). We adopt $\alpha_{\rm CE} = \alpha_{\rm th} = 0.75$ in our standard model, and $\alpha_{\rm CE} = \alpha_{\rm th} = 1.0$ to investigate the effect of varying the CE ejection parameters.

The WD binary formed from the first RLOF phase continues to evolve, and the secondary may fill its Roche lobe as a red giant. The system then experiences a second RLOF phase. If the mass ratio at the onset of RLOF is greater than $q_{\rm crit}$ given in table 3 of Han et al. (2002), RLOF is dynamically unstable, leading again to a CE phase. If the CE is ejected, a hot subdwarf star may be formed. The hot subdwarf binary has a short orbital period and a WD companion (*2nd CE channel* for the formation of hot subdwarfs). However, RLOF may be stable if the mass ratio is sufficiently small. In this case, we assume that the mass lost from the mass donor is all lost from the system, carrying away the same specific angular momentum as pertains to the WD companion. Stable RLOF may then result in the formation of a hot subdwarf binary with a WD companion and a long orbital period (typically $\sim 1000\,{\rm d}$, *2nd stable RLOF channel* for the formation of hot subdwarfs).

If the second RLOF phase results in a CE phase and the CE is ejected, a double white dwarf system is formed (Webbink 1984; Iben & Tutukov 1986; Han 1998). Some of the double WD systems contain two helium WDs. Angular momentum loss due to gravitational wave radiation may then cause the shrinking of the orbital separation until the less massive white dwarf starts to fill its Roche lobe. This will lead to its dynamical disruption if

$$q \gtrsim 0.7 - 0.1(M_2/\,M_\odot) \qquad (2)$$

or $M_1 \gtrsim 0.3\,M_\odot$, where M_1 is the mass of the donor (i.e. the less massive WD) and M_2 is the mass of the gainer (Han & Webbink 1999). This is expected to always lead to a complete merger of the two white dwarfs. The merger can also produce a hot subdwarf star, but in this case the hot subdwarf star is a single object (*He WD merger channel* for the formation of hot subdwarfs). If the lighter WD is not disrupted, RLOF is stable and an AM CVn system is formed.

In this paper, we do not include a tidally enhanced stellar wind explicitly as was done in Han et al. (1995) and Han (1998). Instead we use a standard Reimers wind formula (Reimers 1975) with $\eta = 1/4$ (Renzini 1981; Iben & Renzini 1983; Carraro et al. 1996) which is included in our stellar models. This is to keep the simulations as simple as possible, although the effects of a tidally enhanced wind can to some degree be implicitly included by using a larger value of $q_{\rm crit}$. We also employ a standard magnetic braking law (Verbunt & Zwaan 1981; Rappaport, Verbunt & Joss 1983) where appropriate (see Podsiadlowski, Han & Rappaport 2002 for details and further discussion).

2.2 Monte-Carlo simulation parameters

In order to investigate the UV-upturn phenomenon due to hot subdwarfs, we have performed a series of Monte-Carlo simulations where we follow the evolution of a sample of a million binaries (single stars are in effect treated as very wide binaries that do not interact with each other), including the hot subdwarfs produced in the simulations, according to our grids of stellar models. The simulations require as input the star formation rate (SFR), the initial mass function (IMF) of the primary, the initial mass-ratio distribution and the distribution of initial orbital separations.

(1) The SFR is taken to be a single starburst in most of our simulations; all the stars have the same age ($t_{\rm SSP}$) and the same metallicity ($Z = 0.02$), and constitute a simple stellar population (SSP). In some simulations a composite stellar population (CSP) is also used (Section 3.3).

(2) A simple approximation to the IMF of Miller & Scalo (1979) is used; the primary mass is generated with the formula of Eggleton, Fitchett & Tout (1989),

$$M_1 = \frac{0.19X}{(1-X)^{0.75} + 0.032(1-X)^{0.25}}, \qquad (3)$$

where X is a random number uniformly distributed between 0 and 1. The adopted range of primary masses is 0.8 to $100.0\,M_\odot$. The studies by Kroupa, Tout & Gilmore (1993) and Zoccali et al. (2000) support this IMF.

(3) The mass-ratio distribution is quite uncertain. We mainly take a constant mass-ratio distribution (Mazeh et al. 1992; Goldberg & Mazeh 1994; Heacox 1995; Halbwachs, Mayor & Udry 1998; Shatsky & Tokovinin 2002),

$$n(q') = 1, \qquad 0 \le q' \le 1, \qquad (4)$$

where $q' = 1/q = M_2/M_1$. As alternatives we also consider a rising mass ratio distribution

$$n(q') = 2q', \qquad 0 \le q' \le 1, \qquad (5)$$

and the case where both binary components are chosen randomly and independently from the same IMF.

(4) We assume that all stars are members of binary systems and that the distribution of separations is constant in $\log a$ (where a is the orbital separation) for wide binaries and falls off smoothly at close separations:

$$an(a) = \begin{cases} \alpha_{\rm sep}(\frac{a}{a_0})^m, & a \le a_0; \\ \alpha_{\rm sep}, & a_0 < a < a_1, \end{cases} \qquad (6)$$

where $\alpha_{\rm sep} \approx 0.070$, $a_0 = 10\,R_\odot$, $a_1 = 5.75 \times 10^6\,R_\odot = 0.13\,{\rm pc}$, and $m \approx 1.2$. This distribution implies that there is an equal number of wide binary systems per logarithmic interval and that approximately 50 per cent of stellar systems are binary systems with orbital periods less than 100 yr.

2.3 Spectral library

In order to obtain the colours and the spectral energy distribution (SED) of the populations produced by our simulations, we have calculated spectra for hot subdwarfs using plane-parallel static model stellar atmospheres computed with the ATLAS9 stellar atmosphere code (Kurucz 1992) with the assumption of local thermodynamic equilibrium (LTE). Solar metal abundances were adopted (Anders & Grevesse 1989) and line blanketing is approximated by appropriate opacity distribution functions interpolated for the chosen helium abundance. The resulting model atmosphere grid covers a wide range of effective temperatures ($10,000 \leq T_{\rm eff} \leq 40,000$K with a spacing of $\Delta T = 1000$K), gravities ($5.0 \leq \log g \leq 7.0$ with $\Delta \log g = 0.2$), and helium abundances ($-3 \leq [He/H] \leq 0$), as appropriate for the hot subdwarfs produced in the BPS code. For the spectrum and colours of other single stars, we use the latest version of the comprehensive BaSeL library of theoretical stellar spectra (see Lejeune et al. 1997, 1998 for a description), which gives the colours and SEDs of stars with a wide range of Z, $\log g$ and $T_{\rm eff}$.

2.4 Observables from the model

Our model follows the evolution of the integrated spectra of stellar populations. In order to compare the results with observations, we calculate the following observables as well as UBV colours in the Johnson system (Johnson & Morgan 1953).

(i) $(1550-V)$ is a colour defined by BBBFL. It is a combination of the short-wavelength IUE flux and the V magnitude and is used to express the magnitude of the UV-upturn:

$$(1550-V) = -2.5\log(f_{\lambda,1250-1850}/f_{\lambda,5055-5945}), \quad (7)$$

where $f_{\lambda,1250-1850}$ is the energy flux per unit wavelength averaged between 1250 and 1850Å and $f_{\lambda,5055-5945}$ the flux averaged between 5055 and 5945Å (for the V band):

(ii) $(1550-2500)$ is a colour defined for the IUE flux by Dorman, O'Connell & Rood (1995).

$$(1550-2500) = -2.5\log(f_{\lambda,1250-1850}/f_{\lambda,2200-2800}). \quad (8)$$

(iii) $(2000-V)$ is a colour used by Deharveng, Boselli & Donas (2002) in their study of UV properties of the early-type galaxies observed with the balloon-borne FOCA experiment (Donas et al. 1990; Donas, Milliard & Laget 1995):

$$(2000-V) = -2.5\log(f_{\lambda,1921-2109}/f_{\lambda,5055-5945}). \quad (9)$$

(iv) $(FUV-NUV)_{\rm AB}$, $(FUV-r)_{\rm AB}$, $(NUV-r)_{\rm AB}$ are colours from GALEX and SDSS. GALEX, a NASA Small Explorer mission, has two bands in its ultraviolet (UV) survey: a far-UV band centered on 1530 Å and a near-UV band centered on 2310 Å (Martin et al. 2005; Rich et al. 2005), while SDSS has five passbands, u at 3551 Å, g at 4686 Å, r at 6165 Å, i at 7481 Å, and z at 8931 Å (Fukugita et al. 1996; Gunn et al. 1998; Smith et al. 2002). The magnitudes are in the AB system of Oke & Gunn (1983):

$$(FUV-NUV)_{\rm AB} = -2.5\log(f_{\nu,1350-1750}/f_{\nu,1750-2750}), \quad (10)$$

$$(FUV-r)_{\rm AB} = -2.5\log(f_{\nu,1350-1750}/f_{\nu,5500-7000}), \quad (11)$$

$$(NUV-r)_{\rm AB} = -2.5\log(f_{\nu,1750-2750}/f_{\nu,5500-7000}), \quad (12)$$

where $f_{\nu,1350-1750}$, $f_{\nu,1750-2750}$, $f_{\nu,5500-7000}$ are the energy fluxes per unit frequency averaged in the frequency bands corresponding to 1350 and 1750 Å, 1750 and 2750 Å, 5500 and 7000 Å, respectively.

(v) $\beta_{\rm FUV}$ is a far-UV spectral index we defined to measure the SED slope between 1075 and 1750 Å:

$$f_\lambda \sim \lambda^{\beta_{\rm FUV}}, \qquad 1075 < \lambda < 1750\,{\rm Å}, \quad (13)$$

where f_λ is the energy flux per unit wavelength. In this paper, we fit far-UV SEDs with equation (13) to obtain $\beta_{\rm FUV}$. In the fitting we ignored the part between 1175 and 1250Å for the theoretical SEDs from our model, as this part corresponds to the L_α line. We also obtained $\beta_{\rm FUV}$ via a similar fitting for early-type galaxies observed with the HUT (Brown et al. 1997; Brown 2004) and the IUE (Burstein et al. 1988). We again ignored the part between 1175 and 1250Å for the HUT SEDs, while the IUE SEDs do not have any data points below 1250Å.

Table 1. Simulation sets (metallicity $Z = 0.02$)

Set	$n(q')$	$q_{\rm c}$	$\alpha_{\rm CE}$	$\alpha_{\rm th}$
Standard SSP simulation set with $t_{\rm SSP}$ varying upto 15 Gyr				
1	constant	1.5	0.75	0.75
SSP simulation sets with varying model parameters				
2	uncorrelated	1.5	0.75	0.75
3	rising	1.5	0.75	0.75
4	constant	1.2	0.75	0.75
5	constant	1.5	1.0	1.0
CSP simulation sets with a $t_{\rm major}$ and variable $t_{\rm minor}$ and f				
6	constant	1.5	0.75	0.75

Note - $n(q')$ = initial mass-ratio distribution; $q_{\rm c}$ = the critical mass ratio above which the first RLOF on the FGB or AGB is unstable; $\alpha_{\rm CE}$ = CE ejection efficiency; $\alpha_{\rm th}$ = thermal contribution to CE ejection; $t_{\rm SSP}$ = the age of a SSP; $t_{\rm major}$ = the age of the major population in a CSP; $t_{\rm minor}$ = the age of the minor population in a CSP; f = the ratio of the mass of the minor population to the total mass in a CSP.

3 SIMULATIONS

In order to investigate the UV-upturn systematically, we performed six sets of simulations for a Population I composition ($X = 0.70$, $Y = 0.28$ and $Z = 0.02$). The first set is a standard set with the best-choice model parameters from HPMM. In Sets 2 to 5 we systematically vary the model parameters, and Set 6 models a composite stellar population (Table 1).

3.1 Standard simulation set

In the HPMM model, hot subdwarfs are produced through binary interactions by stable RLOF, CE ejection or He WD mergers. The main parameters in the HPMM model are: $n(q')$, the initial mass ratio distribution, $q_{\rm c}$, the critical mass ratio above which the 1st RLOF on the FGB or AGB is unstable, $\alpha_{\rm CE}$, the CE ejection efficiency parameter, and $\alpha_{\rm th}$, the contribution of thermal energy to the binding energy of the CE (see Sections 2.1 and 2.2 for details). The model that best reproduces the observed properties of hot subdwarfs in our Galaxy has $n(q') = 1$, $q_{\rm c} = 1.5$, $\alpha_{\rm CE} = 0.75$, $\alpha_{\rm th} = 0.75$, (see section 7.4 of Han et al. 2003). These are the parameters adopted in our standard simulation.

In our standard set, we first construct a SSP containing a million binaries (Section 2.2). The binaries are formed simultaneously (i.e. in a single starburst) and with the same metallicity ($Z = 0.02$). The SSP is evolved with the BPS code (Section 2.1), and the results are convolved with our spectral libraries (Section 2.3) to produce integrated SEDs and other observables. The SEDs are normalised to a stellar population of mass $10^{10} M_{\odot}$ at a distance of 10 Mpc.

3.2 Simulation sets with varying model parameters

In order to investigate the importance of the model parameters, we also carried out simulation sets in which we systematically varied the main parameters. Specifically, we adopted three initial mass-ratio distributions: a constant mass-ratio distribution, a rising mass-ratio distribution, and one where the component masses are uncorrelated and drawn independently from a Miller-Scalo IMF (Section 2.2). We also varied the value of $q_{\rm c}$ in the instability criterion for the first RLOF phase on the FGB or AGB from 1.5 to 1.2, the parameter $\alpha_{\rm CE}$ for CE ejection efficiency and the parameter $\alpha_{\rm th}$ for the thermal contribution to CE ejection from 0.75 to 1.0.

3.3 Simulation sets for composite stellar populations

Many early-type galaxies show evidence for some moderate amount of recent star formation (Yi et al. 2005; Salim et al. 2005; Schawinski et al. 2006). Therefore, we also perform simulations in which we evolve composite stellar populations. Here, a composite stellar population (CSP) consists of two populations, a major old one and a minor younger one. The major population has solar metallicity and an age of $t_{\rm major}$, where all stars formed in a single burst $t_{\rm major}$ ago, while the minor one has solar metallicity and an age $t_{\rm minor}$, where all stars formed in a starburst starting $t_{\rm minor}$ ago and lasting 0.1 Gyr. The minor population fraction f is the ratio of the mass of the minor population to the total mass of the CSP (for $f = 100\%$ the CSP is actually a SSP with an age $t_{\rm minor}$).

4 RESULTS AND DISCUSSION

4.1 Simple stellar populations

4.1.1 Evolution of the integrated SED

In our standard simulation set, we follow the evolution of the integrated SED of a SSP (including binaries) of $10^{10} M_{\odot}$ up to $t_{\rm SSP} = 15\,{\rm Gyr}$. The SSP is assumed to be at a distance of 10 Mpc and the evolution is shown in Figure 2. Note that hot subdwarfs originating from binary interactions start to dominate the far-UV after $\sim 1\,{\rm Gyr}$.

We have compiled a file containing the spectra of the SSP with ages from 0.1 Gyr to 15 Gyr and devised a small FORTRAN code to read the file (and to plot the SEDs with PGPLOT). The file and the code are available online[2]. In order to be able to apply the model directly, we have also provided in the file the spectra of the SSP without any binary interactions considered. This provides an easy way to examine the differences in the spectra for simulations with and without binary interactions.

[2] The file and the code are available on the VizieR data base of the astronomical catalogues at the Centre de Données astronomiques de Strasbourg (CDS) web site (http://cdsarc.u-strasbg.fr/) and on ZH's personal website (http://www.zhanwenhan.com/download/uv-upturn.html).

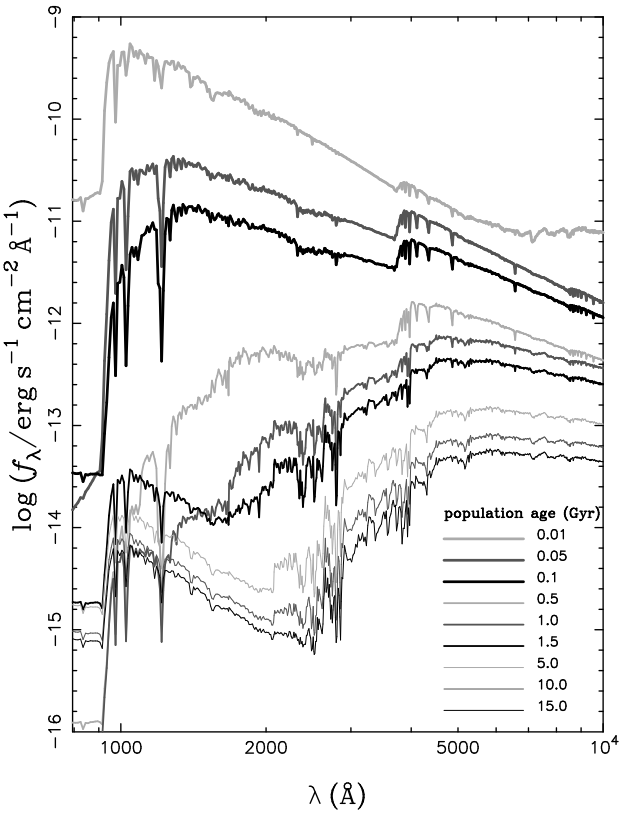

Figure 2. The evolution of the restframe intrinsic spectral energy distribution (SED) for a simulated galaxy in which all stars formed at the same time, representing a simple stellar population (SSP). The stellar population (including binaries) has a mass of $10^{10} M_{\odot}$ and the galaxy is assumed to be at a distance of 10 Mpc. The figure is for the standard simulation set, and no offset has been applied to the SEDs.

4.1.2 Evolution of the UV-upturn

The colours of the SSP evolve in time, and Table 2 lists the colours of a SSP (including binaries) of $10^{10} M_{\odot}$ at various ages for the standard simulation set. In order to see how the colours evolve with redshift, we adopted a ΛCDM cosmology (Carroll, Press & Turner 1992) with cosmological parameters of $H_0 = 72{\rm km/s/Mpc}$, $\Omega_{\rm M} = 0.3$ and $\Omega_{\Lambda} = 0.7$, and assumed a star-formation redshift of $z_{\rm f} = 5$ to obtain Figures 3 and 4. The figures show the evolution of the restframe intrinsic colours and the evolution of the far-UV spectral index with redshift (look-back time). As these figures show, the UV-upturn does not evolve much with redshift; for an old stellar population (i.e. with a redshift $z \sim 0$ or an age of $\sim 12\,{\rm Gyr}$), $(1550 - V) \sim 3.5$, $(UV - V) \sim 4.4$, $(FUV - r)_{\rm AB} \sim 6.7$, $(1550 - 2500) \sim -0.38$, $(FUV - NUV)_{\rm AB} \sim 0.42$ and $\beta_{\rm FUV} \sim -3.0$.

4.1.3 Colour-colour diagrams

Colour-colour diagrams are widely used as a diagnostic tool in the study of stellar populations of early-type galaxies. We present a few such diagrams in Figures 5 and 6 for the standard simulation set. In these figures, most curves have a turning-point at $\sim 1\,{\rm Gyr}$, at which hot subdwarfs resulting from binary interactions start to dominate the far-UV.

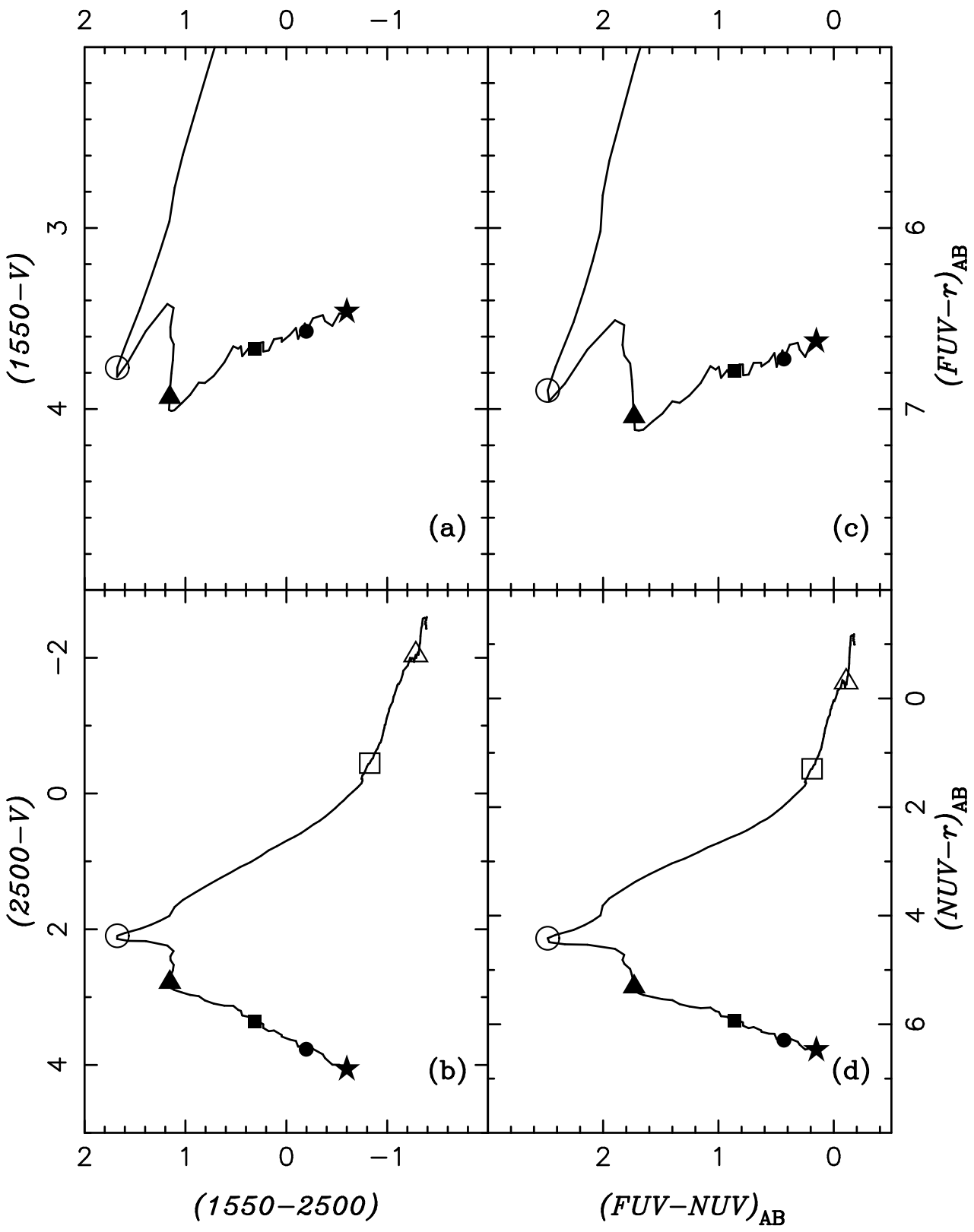

Figure 5. Colour-colour diagrams for the standard simulation set. Ages are denoted by open triangles (0.01 Gyr), open squares (0.1 Gyr), open circles (1 Gyr), filled triangles (2 Gyr), filled squares (5 Gyr), filled circles (10 Gyr) and filled stars (15 Gyr).

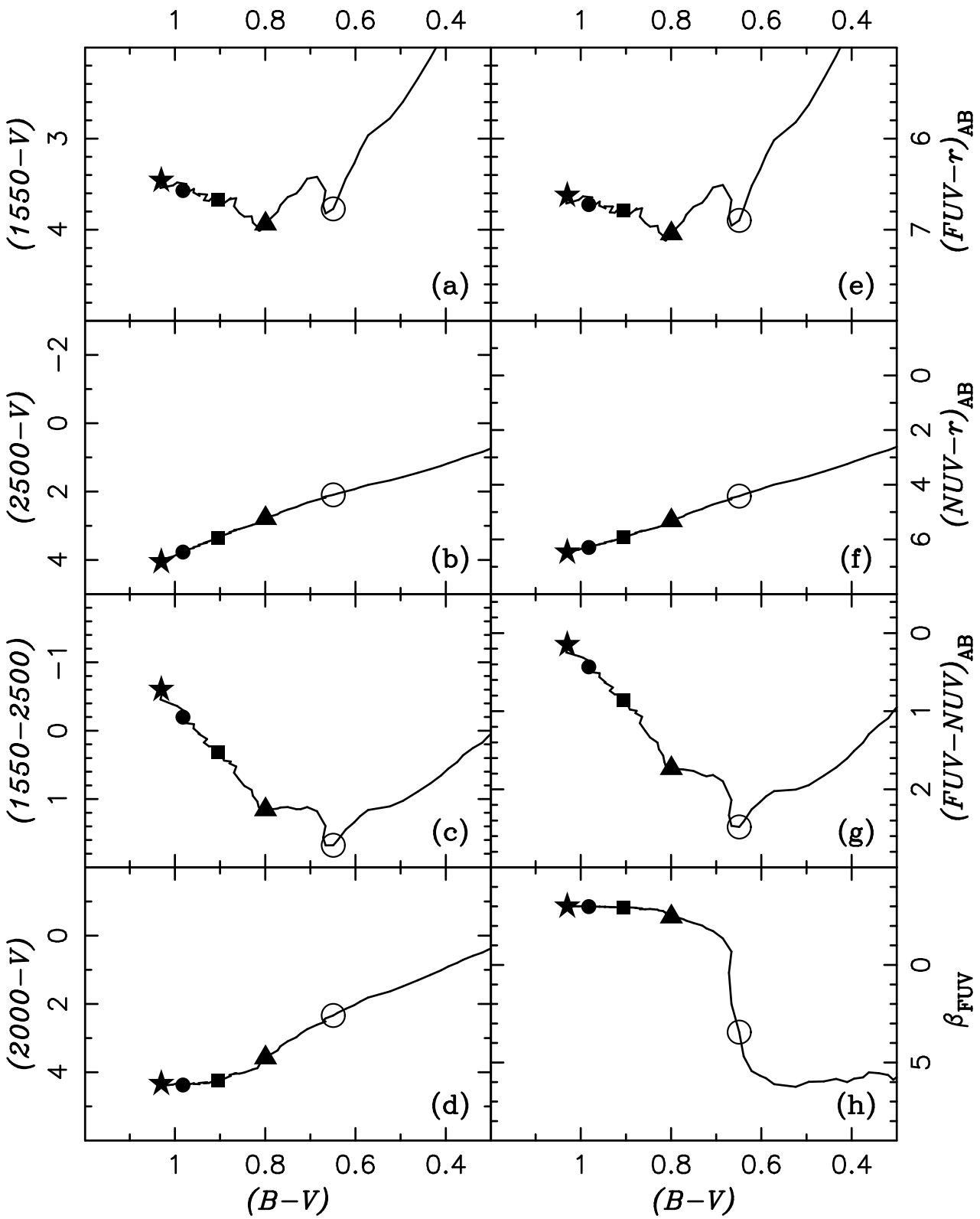

Figure 6. Similar to Figure 5, but with $(B-V)$ as the abscissa.

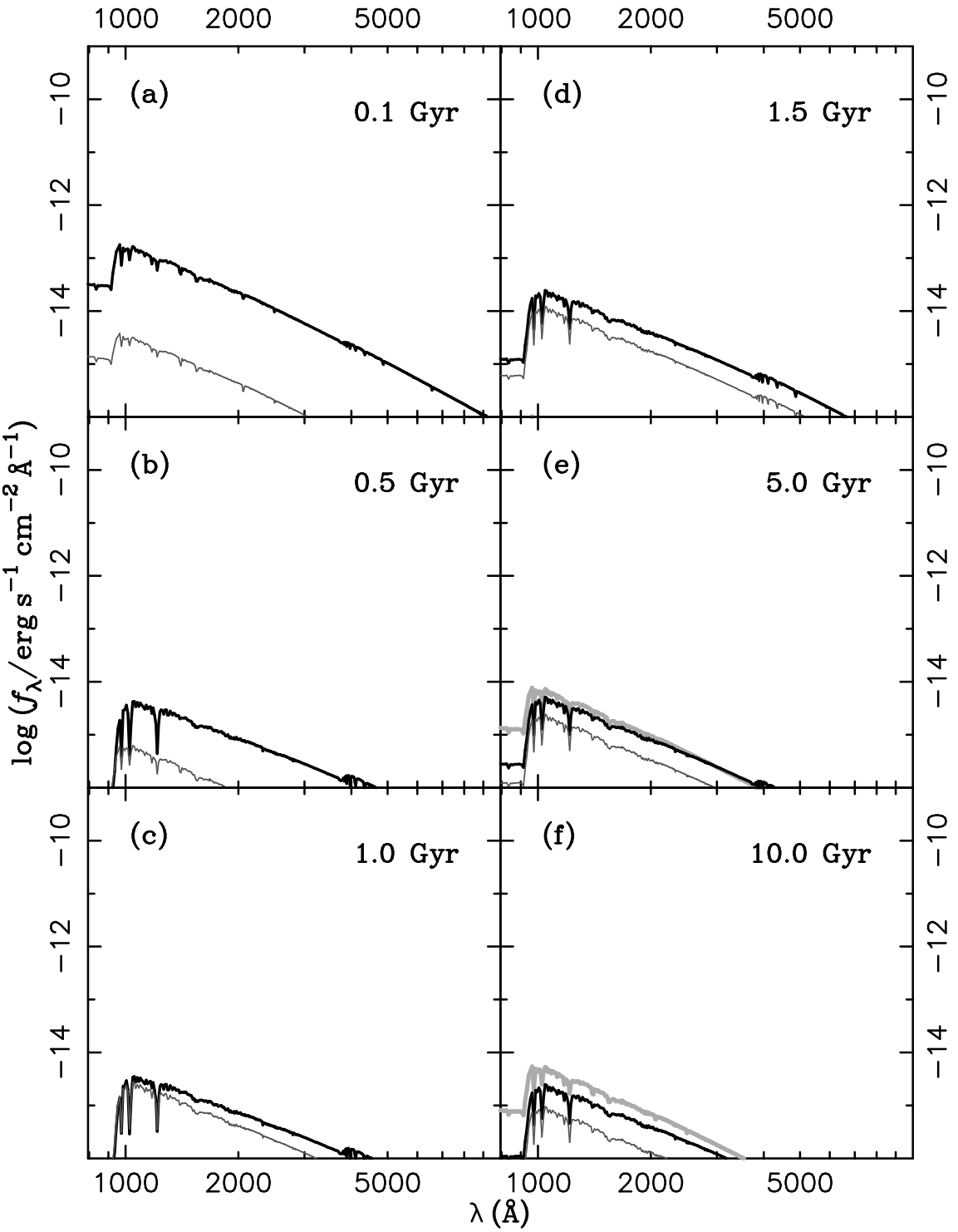

Figure 7. Integrated restframe intrinsic SEDs for hot subdwarfs for different formation channels. Solid, thin dark grey and thick light grey curves are for the stable RLOF channel, the CE ejection channel and the merger channel, respectively. The merger channel starts to dominate at an age of $t_{\rm SSP} \sim 3.5\,{\rm Gyr}$. The figure is for the standard simulation set with a stellar population mass of $10^{10} M_\odot$ (including binaries), and the population is assumed to be at a distance of 10 Mpc.

Table 2. Colour evolution of a simple stellar population (including binaries) of $10^{10}\,M_{\odot}$ for the standard simulation set. This table is also available in machine-readable form on the VizieR data base of the astronomical catalogues at the Centre de Données astronomiques de Strasbourg (CDS) web site (http://cdsarc.u-strasbg.fr/) and on ZH's personal website (http://www.zhanwenhan.com/download/uv-upturn.html).

$\log(t_{\rm SSP})$	$M_{\rm V}$	$B-V$	$15-V$	$20-V$	$25-V$	$15-25$	$FUV-r$	$NUV-r$	$FUV-NUV$	$\beta_{\rm FUV}$
-1.000	-22.416	0.173	-1.274	-0.953	-0.447	-0.827	1.483	1.296	0.188	0.775
-0.975	-22.346	0.165	-1.245	-0.938	-0.432	-0.813	1.503	1.304	0.199	0.941
-0.950	-22.306	0.175	-1.195	-0.901	-0.396	-0.799	1.555	1.346	0.209	1.100
-0.925	-22.289	0.185	-1.106	-0.829	-0.326	-0.780	1.644	1.421	0.223	1.305
-0.900	-22.232	0.194	-1.053	-0.788	-0.286	-0.767	1.699	1.466	0.233	1.479
-0.875	-22.168	0.192	-1.019	-0.766	-0.265	-0.754	1.730	1.487	0.243	1.659
-0.850	-22.135	0.199	-0.959	-0.717	-0.215	-0.744	1.792	1.542	0.250	1.842
-0.825	-22.053	0.199	-0.969	-0.723	-0.216	-0.753	1.780	1.537	0.243	1.968
-0.800	-22.000	0.200	-0.945	-0.701	-0.189	-0.756	1.802	1.561	0.241	2.182
-0.775	-21.949	0.205	-0.892	-0.660	-0.148	-0.744	1.855	1.605	0.250	2.407
-0.750	-21.923	0.207	-0.789	-0.587	-0.086	-0.703	1.955	1.674	0.281	2.656
-0.725	-21.885	0.211	-0.682	-0.514	-0.025	-0.658	2.058	1.743	0.316	2.935
-0.700	-21.839	0.218	-0.569	-0.437	0.041	-0.609	2.169	1.816	0.353	3.314
-0.675	-21.804	0.221	-0.468	-0.367	0.101	-0.569	2.266	1.882	0.384	3.565
-0.650	-21.767	0.223	-0.377	-0.307	0.152	-0.529	2.355	1.939	0.416	3.832
-0.625	-21.732	0.230	-0.272	-0.235	0.215	-0.486	2.459	2.009	0.451	4.087
-0.600	-21.689	0.235	-0.166	-0.167	0.273	-0.439	2.565	2.075	0.490	4.343
-0.575	-21.644	0.242	-0.051	-0.092	0.337	-0.388	2.681	2.148	0.532	4.583
-0.550	-21.606	0.246	0.074	-0.015	0.403	-0.329	2.806	2.222	0.583	4.879
-0.525	-21.546	0.250	0.188	0.048	0.456	-0.268	2.918	2.280	0.638	5.176
-0.500	-21.512	0.263	0.315	0.122	0.522	-0.207	3.055	2.359	0.695	5.384
-0.475	-21.478	0.274	0.444	0.196	0.587	-0.144	3.189	2.433	0.757	5.503
-0.450	-21.424	0.285	0.556	0.254	0.637	-0.081	3.316	2.495	0.820	5.524
-0.425	-21.377	0.292	0.688	0.322	0.694	-0.005	3.458	2.560	0.898	5.603
-0.400	-21.335	0.308	0.872	0.421	0.777	0.095	3.661	2.660	1.001	5.881
-0.375	-21.290	0.319	1.015	0.497	0.840	0.175	3.825	2.736	1.089	5.642
-0.350	-21.253	0.340	1.172	0.591	0.919	0.253	4.011	2.834	1.176	5.545
-0.325	-21.217	0.362	1.374	0.706	1.015	0.360	4.246	2.951	1.295	5.507
-0.300	-21.162	0.375	1.543	0.795	1.084	0.459	4.440	3.036	1.404	5.764
-0.275	-21.121	0.394	1.723	0.903	1.168	0.555	4.651	3.143	1.507	5.827
-0.250	-21.068	0.410	1.897	1.012	1.245	0.653	4.846	3.242	1.604	6.004
-0.225	-21.028	0.434	2.116	1.152	1.344	0.772	5.095	3.374	1.721	5.839
-0.200	-20.994	0.462	2.339	1.305	1.448	0.890	5.343	3.517	1.826	5.968
-0.175	-20.965	0.495	2.597	1.485	1.571	1.026	5.629	3.682	1.947	5.989
-0.150	-20.937	0.524	2.778	1.632	1.671	1.107	5.820	3.816	2.004	6.248
-0.125	-20.930	0.572	2.964	1.814	1.804	1.159	6.018	3.994	2.024	6.113
-0.100	-20.864	0.590	3.123	1.932	1.873	1.250	6.184	4.092	2.091	5.806
-0.075	-20.801	0.603	3.274	2.038	1.933	1.340	6.336	4.174	2.162	5.673
-0.050	-20.730	0.622	3.440	2.142	1.992	1.448	6.522	4.264	2.258	5.434
-0.025	-20.664	0.639	3.655	2.254	2.056	1.599	6.768	4.355	2.413	4.681
0.000	-20.583	0.649	3.771	2.336	2.096	1.675	6.897	4.415	2.482	3.445
0.025	-20.511	0.666	3.822	2.424	2.144	1.677	6.955	4.488	2.467	2.006
0.050	-20.419	0.672	3.737	2.484	2.171	1.566	6.860	4.528	2.332	0.404
0.075	-20.313	0.666	3.569	2.517	2.176	1.393	6.672	4.534	2.137	-0.684
0.100	-20.259	0.685	3.420	2.607	2.241	1.179	6.509	4.612	1.897	-1.360
0.125	-20.201	0.707	3.441	2.738	2.323	1.118	6.536	4.719	1.817	-1.734
0.150	-20.150	0.722	3.547	2.866	2.398	1.149	6.646	4.814	1.832	-1.868
0.175	-20.081	0.731	3.603	2.974	2.455	1.148	6.704	4.888	1.816	-2.019
0.200	-20.028	0.750	3.642	3.094	2.525	1.117	6.748	4.983	1.766	-2.148
0.225	-19.973	0.766	3.731	3.240	2.606	1.125	6.837	5.085	1.752	-2.270

4.1.4 The far-UV contribution for different formation channels of hot subdwarfs

In our model, there are three channels for the formation of hot subdwarfs. In the stable RLOF channel, the hydrogen-rich envelope of a star with a helium core is removed by stable mass transfer, and helium is ignited in the core. The hot subdwarfs from this channel are in binaries with long orbital periods (typically $\sim 1000\,{\rm d}$). In the CE ejection channel, the envelope is ejected as a consequence of the spiral-in in a CE phase. The resulting hot subdwarf binaries have

Table 2. continued

$\log(t_{\rm SSP})$	$M_{\rm V}$	$B-V$	$15-V$	$20-V$	$25-V$	$15-25$	$FUV-r$	$NUV-r$	$FUV-NUV$	$\beta_{\rm FUV}$
0.250	-19.906	0.773	3.804	3.359	2.664	1.140	6.902	5.157	1.745	-2.342
0.275	-19.853	0.790	3.886	3.492	2.735	1.151	6.992	5.254	1.739	-2.457
0.300	-19.789	0.799	3.936	3.571	2.781	1.155	7.042	5.311	1.731	-2.466
0.325	-19.746	0.811	4.005	3.684	2.842	1.162	7.115	5.389	1.726	-2.573
0.350	-19.664	0.812	4.010	3.761	2.870	1.140	7.119	5.428	1.691	-2.680
0.375	-19.588	0.815	4.007	3.821	2.895	1.111	7.113	5.462	1.651	-2.706
0.400	-19.533	0.818	3.968	3.879	2.932	1.036	7.067	5.499	1.568	-2.759
0.425	-19.484	0.827	3.922	3.915	2.968	0.954	7.025	5.539	1.486	-2.787
0.450	-19.412	0.830	3.854	3.931	2.987	0.867	6.957	5.557	1.401	-2.828
0.475	-19.374	0.846	3.856	4.009	3.049	0.807	6.965	5.629	1.336	-2.865
0.500	-19.337	0.857	3.817	4.041	3.096	0.720	6.924	5.673	1.251	-2.851
0.525	-19.288	0.869	3.743	4.041	3.127	0.615	6.857	5.703	1.154	-2.857
0.550	-19.201	0.864	3.653	4.026	3.128	0.525	6.763	5.693	1.070	-2.896
0.575	-19.170	0.879	3.666	4.082	3.189	0.477	6.782	5.758	1.024	-2.914
0.600	-19.089	0.876	3.654	4.103	3.203	0.451	6.767	5.770	0.996	-2.930
0.625	-19.055	0.891	3.708	4.188	3.271	0.437	6.828	5.850	0.978	-2.944
0.650	-18.992	0.896	3.666	4.179	3.290	0.376	6.785	5.862	0.923	-2.925
0.675	-18.957	0.904	3.695	4.230	3.340	0.355	6.817	5.914	0.903	-2.933
0.700	-18.880	0.905	3.667	4.239	3.357	0.310	6.788	5.928	0.860	-2.955
0.725	-18.812	0.906	3.635	4.238	3.371	0.264	6.754	5.936	0.818	-2.962
0.750	-18.758	0.913	3.631	4.247	3.402	0.229	6.754	5.966	0.788	-2.944
0.775	-18.710	0.925	3.682	4.310	3.453	0.229	6.814	6.029	0.785	-2.958
0.800	-18.680	0.936	3.676	4.325	3.502	0.174	6.810	6.071	0.739	-2.956
0.825	-18.576	0.929	3.615	4.290	3.492	0.123	6.745	6.050	0.695	-2.964
0.850	-18.556	0.947	3.606	4.314	3.560	0.046	6.744	6.113	0.631	-2.974
0.875	-18.473	0.945	3.629	4.348	3.583	0.046	6.765	6.138	0.627	-2.979
0.900	-18.429	0.959	3.591	4.338	3.626	-0.035	6.735	6.173	0.562	-2.980
0.925	-18.362	0.958	3.552	4.319	3.647	-0.095	6.691	6.176	0.514	-2.988
0.950	-18.339	0.981	3.613	4.391	3.729	-0.116	6.767	6.271	0.496	-2.986
0.975	-18.236	0.972	3.528	4.322	3.711	-0.184	6.675	6.231	0.445	-2.992
1.000	-18.191	0.982	3.570	4.374	3.768	-0.198	6.724	6.292	0.432	-2.989
1.025	-18.100	0.975	3.499	4.320	3.764	-0.265	6.645	6.263	0.382	-2.998
1.050	-18.100	0.995	3.481	4.321	3.843	-0.362	6.634	6.321	0.313	-3.005
1.075	-18.036	1.004	3.514	4.359	3.898	-0.384	6.672	6.376	0.296	-3.002
1.100	-18.044	1.032	3.541	4.396	3.997	-0.456	6.712	6.465	0.247	-2.998
1.125	-17.947	1.029	3.473	4.338	3.998	-0.525	6.641	6.441	0.201	-2.999
1.150	-17.884	1.033	3.473	4.345	4.039	-0.566	6.641	6.468	0.173	-2.995
1.175	-17.800	1.030	3.463	4.338	4.062	-0.600	6.626	6.475	0.151	-2.995

Note - $t_{\rm SSP}$ = population age in Gyr; $M_{\rm V}$ = absolute visual magnitude; $B-V$ = $(B-V)$; $15-V$ = $(1550-V)$; $20-V$ = $(2000-V)$; $25-V$ = $(2500-V)$; $15-25$ = $(1550-2500)$; $FUV-r$ = $(FUV-r)_{\rm AB}$; $NUV-r$ = $(FUV-r)_{\rm AB}$; $FUV-NUV$ = $(FUV-NUV)_{\rm AB}$; $\beta_{\rm FUV}$ = far-UV spectral index.

very short orbital periods (typically $\sim 1\,{\rm d}$). In the merger channel, a helium WD pair coalesces to produce a single object. Hot subdwarfs from the merger channel are generally more massive than those from stable RLOF channel or the CE channel and have much thinner (or no) hydrogen envelope. They are therefore expected to be hotter. See Han et al. (2002; 2003) for further details.

Figure 7 shows the SEDs of the hot subdwarfs produced from the different formation channels at various ages. It shows that hot subdwarfs from the RLOF channel are always important, while the CE channel becomes important at an age of $\sim 1\,{\rm Gyr}$. The merger channel, however, catches up with the CE channel at $\sim 2.5\,{\rm Gyr}$ and the stable RLOF channel at $\sim 3.5\,{\rm Gyr}$, and dominates the far-UV flux afterwards.

4.1.5 The effects of the model assumptions

In order to systematically investigate the dependence of the UV-upturn on the parameters of our model, we now vary the major model parameters: $n(q')$ for the initial mass-ratio distribution, $q_{\rm c}$ for the critical mass ratio for stable RLOF on the FGB or AGB, $\alpha_{\rm CE}$ for the CE ejection efficiency and $\alpha_{\rm th}$ for the thermal contribution to the CE ejection. We carried out four more simulation sets (Table 1). Figures 3 and 4 show the UV-upturn evolution of the various simulation sets. These figures show that the initial mass-ratio distribution is very important. As an extreme case, the mass-ratio distribution for uncorrelated component masses (Set 2) makes the UV-upturn much weaker, by $\sim 1{\rm mag}$ in $(1550-V)$ or $(FUV-r)_{\rm AB}$, as compared to the standard simulation set. On the other hand, a rising distribution (Set 3) makes the UV-upturn stronger. Binaries with a mass-ratio distribution of uncorrelated

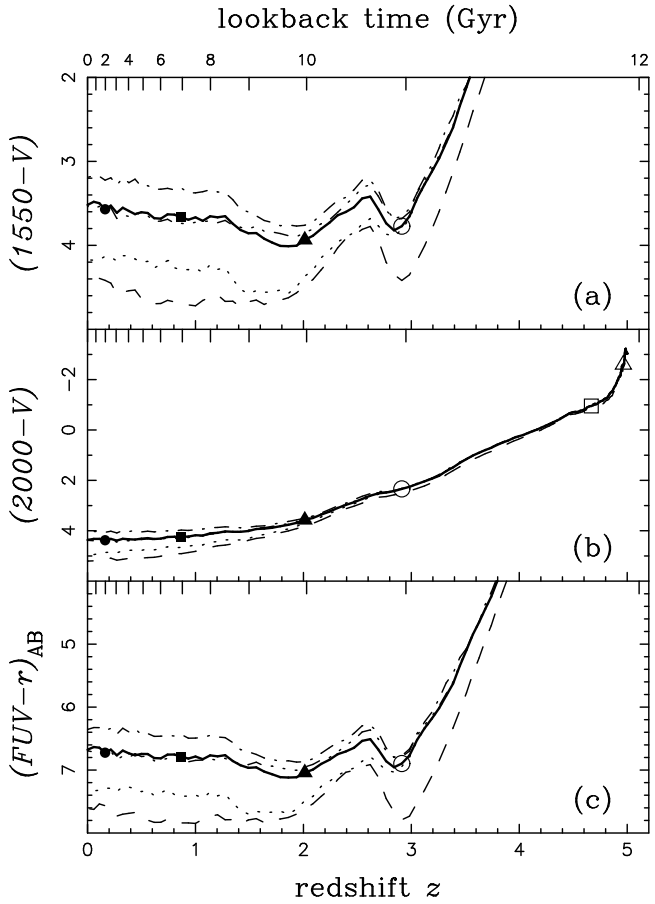

Figure 3. The evolution of restframe intrinsic colours $(1550-V)$, $(2000-V)$ and $(FUV-r)_{\rm AB}$ with redshift (lookback time) for a simple stellar population (including binaries). Solid, dashed, dash-dotted, dotted, dash-dot-dot-dot curves are for simulation sets 1 (standard set), 2, 3, 4, 5, respectively. Ages are denoted by open triangles (0.01 Gyr), open squares (0.1 Gyr), open circles (1 Gyr), filled triangles (2 Gyr), filled squares (5 Gyr) and filled circles (10 Gyr).

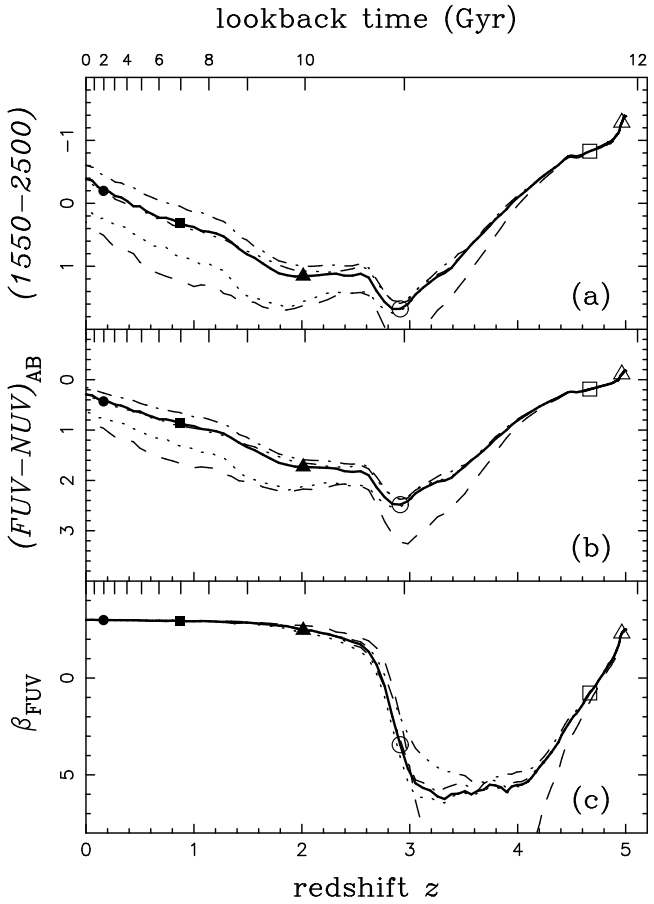

Figure 4. Similar to Figure 3, but for colours $(1550-2500)$, $(FUV-NUV)_{\rm AB}$, and far-UV spectral index $\beta_{\rm FUV}$.

component masses tend to have bigger values of q (the ratio of the mass of the primary to the mass of the secondary), and mass transfer is more likely to be unstable. As a result, the numbers of hot subdwarfs from the stable RLOF channel and the merger channel are greatly reduced, and the UV-upturn is smaller in strength. Binaries with a rising mass-ratio distribution tend to have smaller values of q and therefore produce a larger UV-upturn. A lower $q_{\rm c}$ (Set 4) leads to a weaker UV-upturn, as the numbers of hot subdwarfs from the stable RLOF channel and the merger channel are reduced. A higher CE ejection efficiency $\alpha_{\rm CE}$ and a higher thermal contribution factor $\alpha_{\rm th}$ (Set 5) result in an increase in the number of hot subdwarfs from the CE channel, but a decrease in the number from the merger channel, and the UV-upturn is not affected much as a consequence.

4.1.6 The importance of binary interactions

Binaries evolve differently from single stars due to the occurrence of mass transfer. Mass transfer may prevent mass donors from evolving to higher luminosity and can produce hotter objects than expected in a single-star population of a certain age (mainly hot subdwarfs and blue stragglers[3]). To demonstrate the importance of binary interactions for the UV-upturn explicitly, we plotted SEDs of a population for two cases in Figure 8. Case 1 (solid curves) is for our standard simulation set, which includes various binary interactions, while case 2 (light grey curves) is for a population of the same mass without any binary interactions. The figure shows that the hot subdwarfs produced by binary interactions are the dominant contributors to the far-UV for a population older than $\sim 1\,{\rm Gyr}$. Note, however, that blue stragglers resulting from binary interactions are important contributors to the far-UV between 0.5 Gyr and 1.5 Gyr.

In order to assess the importance of binary interactions for the UV upturn, we define factors that give the fraction of the flux in a particular waveband that originates from hot subdwarfs produced in binaries: $b_{\rm FUV} = F^{\rm sd}_{\rm FUV}/F^{\rm total}_{\rm FUV}$, where $F^{\rm sd}_{\rm FUV}$ is the integrated flux between 900Å and 1800Å radiated by hot subdwarfs (and their descendants) produced by binary interactions, and $F^{\rm total}_{\rm FUV}$ is the total integrated flux between 900Å and 1800Å . We also defined other similar factors, b_{1550}, b_{2000}, and b_{2500}, for passbands of 1250Å to 1850Å , 1921Å to 2109Å, and 2200Å to 2800Å, respectively. Figure 9 shows the time evolution of those factors. As

[3] Blue stragglers are stars located on the main sequence well beyond the turning-point in the colour-magnitude diagram of globular clusters (Sandage 1953), which should already have evolved off the main sequence. Collisions between low-mass stars and mass transfer in close binaries are believed to be responsible for the production of these hotter objects (e.g. Pols & Marinus 1994, Chen & Han 2004, Hurley et al. 2005).

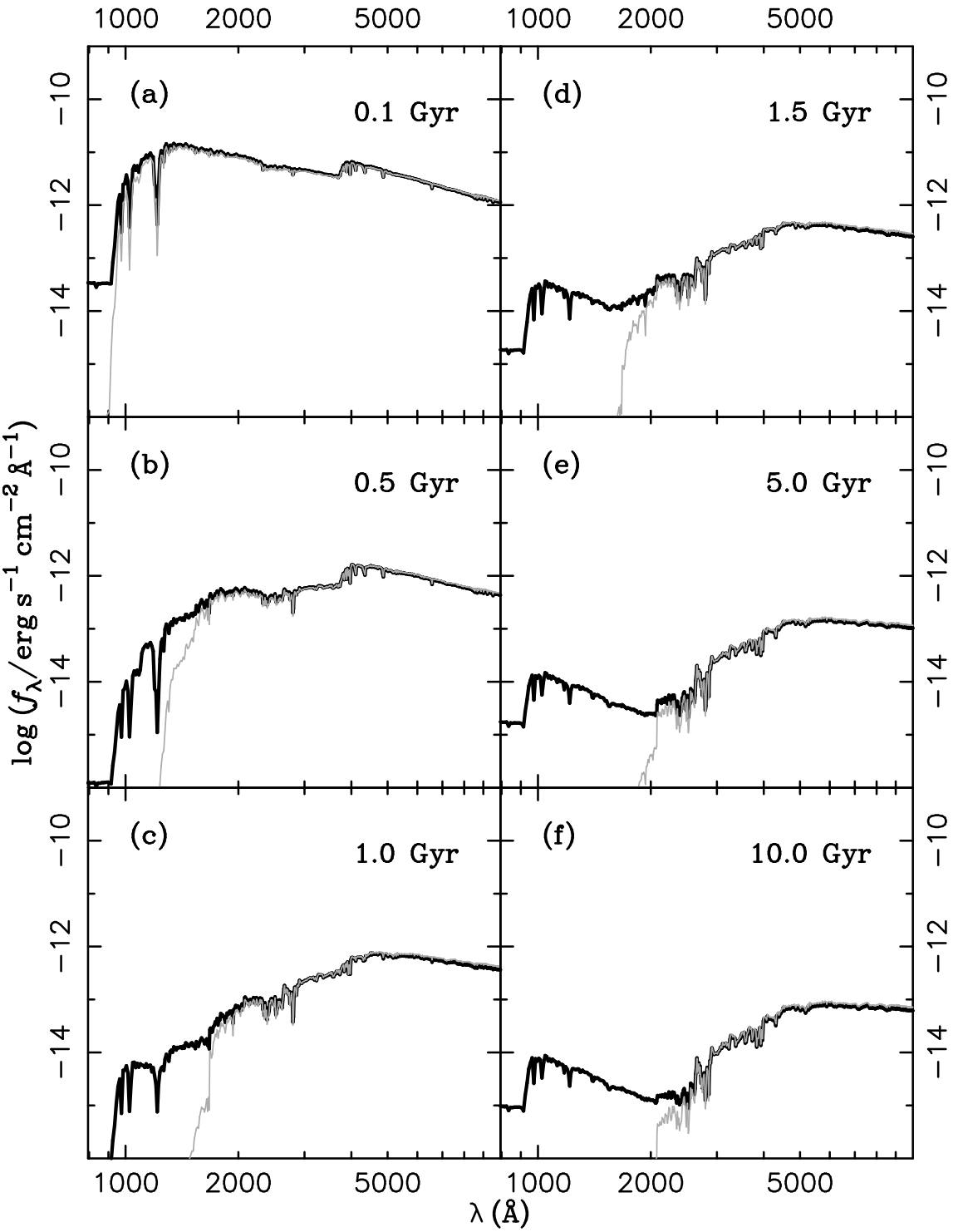

Figure 8. Integrated restframe intrinsic SEDs for a stellar population (including binaries) with a mass of $10^{10} M_{\odot}$ at a distance of 10 Mpc. Solid curves are for the standard simulation set with binary interactions included, and the light grey curves for the same population, but no binary interactions are considered; the two components evolve independently.

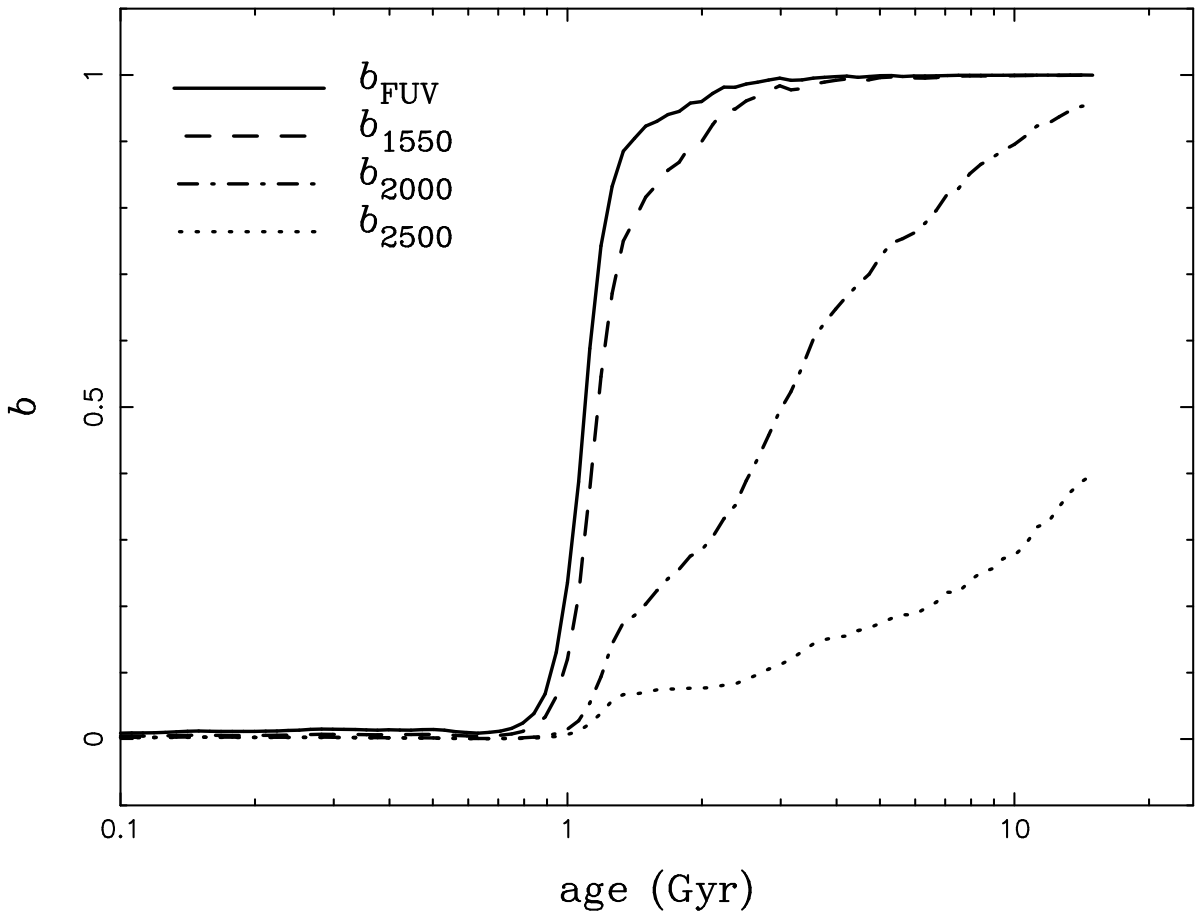

Figure 9. Time evolution of the fraction of the energy flux in different UV wavebands originating from hot subdwarfs (and their descendants) formed in binaries for the standard simulation set.

the figure shows, the hot-subdwarf contribution becomes increasingly important in the far- and near-UV as the population ages.

4.2 The model for composite stellar populations

Early-type galaxies with a recent minor starburst can be modelled as a composite stellar population (CSP). A CSP contains a major population with an age of $t_{\rm major}$ and a minor population of age $t_{\rm minor}$ and mass fraction f (Section 3.3). Figure 10 shows the colour–colour diagram for CSPs with $t_{\rm major} = 10\,{\rm Gyr}$ with varying $t_{\rm minor}$ and f. Note that the curves of different f start to converge to the SSP curve, the curve of $f = 100\%$, for $t_{\rm minor} > 1\,{\rm Gyr}$. This implies that there exists a strong degeneracy between the age of the minor population and the mass fraction.

4.3 Theory versus observations

4.3.1 The fitting of the far-UV SED

In our binary population synthesis model, we adopted solar metallicity. To test the model, we chose NGC 3379, a typical elliptical galaxy with a metallicity close to solar (Gregg et al. 2004) to fit the far-UV SED. Figure 11 presents various fits that illustrate the effects of different sub-populations with different ages and different amounts of assumed extinction. As the figure shows, acceptable fits can be obtained for the various cases. Our best fits require the presence of a sub-population of relatively young stars with an age $< 0.5\,{\rm Gyr}$, making up $\sim 0.1\,\%$ of the total population mass.

The existence of a relatively young population could imply the existence of some core-collapse supernovae in these galaxies. If we assume that an elliptical galaxy has a stellar mass of $10^{11} M_{\odot}$ and 0.1% of the mass was formed *during* the last 0.4 Gyr, then a mean star formation rate would be $0.25 M_{\odot}/{\rm yr}$, about one tenth that of the Galaxy. Core-collapse supernovae would be possible. Indeed, a Type Ib supernova, SN 2000ds, was discovered in NGC 2768, an elliptical galaxy of type E6 (Van Dyk, Li & Filippenko 2003).

4.3.2 The UV-upturn magnitudes versus the far-UV spectral index

There is increasing evidence that many elliptical galaxies had some recent minor star-formation events (Schawinski et al. 2006; Kaviraj et al. 2006), which also contribute to the far-UV excess. To model such secondary minor starbursts, we have constructed CSP galaxy models, consisting of one old, dominant population with an assumed age $t_{\rm major} = 10\,{\rm Gyr}$ and a younger population of variable age, making up a fraction f of the stellar mass of the system. Our spectral modelling shows that a recent minor starburst mostly affects the slope in the far-UV SED, and we therefore defined a far-UV slope index $\beta_{\rm FUV}$ (Section 2.4). In order to assess the importance of binary interactions, we also defined a binary contribution

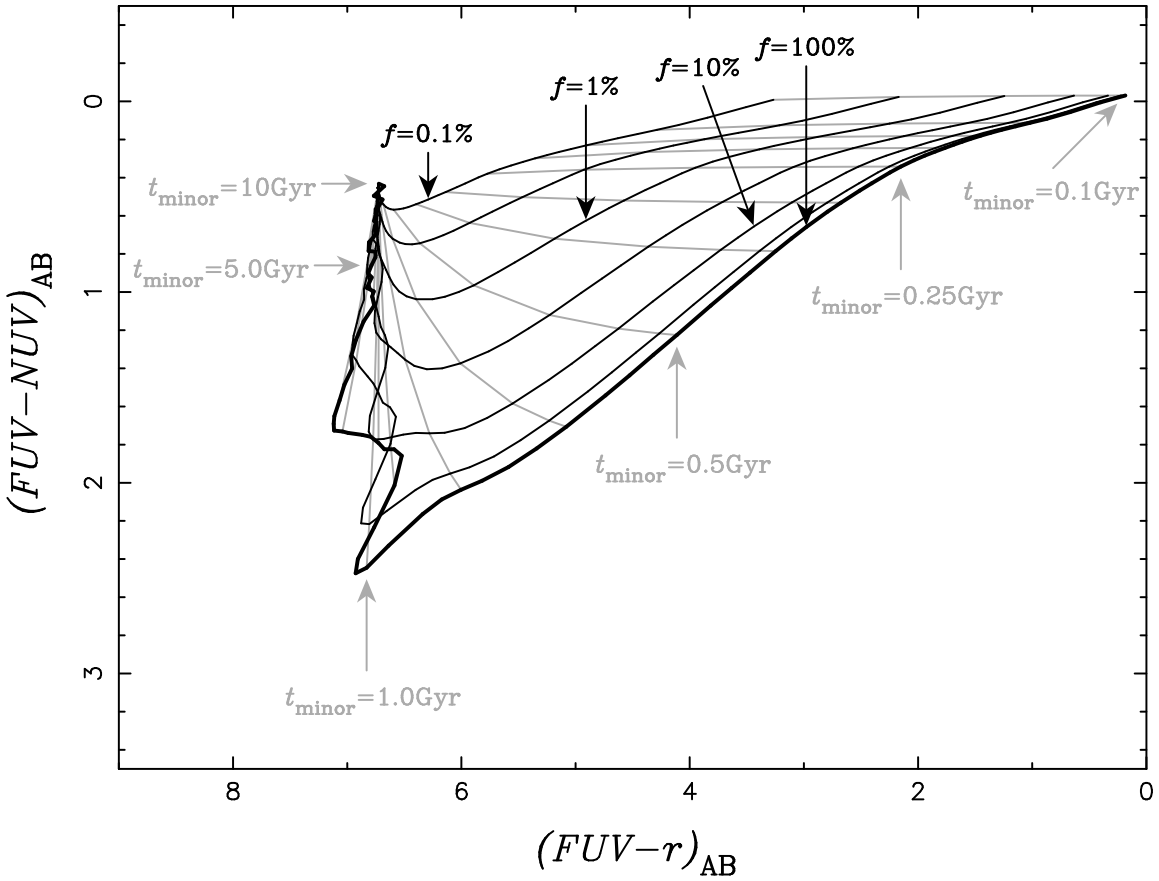

Figure 10. The diagram of $(FUV-NUV)_{\rm AB}$ versus $(FUV-r)_{\rm AB}$ for a composite stellar population (CSP) model of elliptical galaxies with a major population age of $t_{\rm major}=10\,$Gyrs (Set 6). Solid curves are for given minor population fractions f and are plotted in steps of $\Delta\log(f)=0.5$, as indicated. Light grey curves are for fixed minor population ages $t_{\rm minor}$ and are plotted in steps of $\Delta\log(t_{\rm minor}/{\rm Gyr})=0.1$, as indicated. The colours are presented in the restframe. The thick solid curve for $f=100\%$ actually shows the evolution of a simple stellar population with age $t_{\rm minor}$.

factor $b_{\rm FUV}$ (Section 4.1.6), which is the fraction of far-UV flux radiated by hot subdwarfs produced by binary interactions.

Figure 12 shows the far-UV slope as a function of UV excess, a potentially powerful diagnostic diagram which illustrates how the UV properties of elliptical galaxies evolve with time in a dominant old population with a young minor sub-population. For comparison, we also plot observed elliptical galaxies. Some of the observed galaxies are from Astro-2 observations with an aperture of $10''\times56''$ (Brown et al. 1997), some are from IUE observations with an aperture of $10''\times20''$ (Burstein et al. 1988). The value of $\beta_{\rm FUV}$ for NGC 1399, however, is derived from Astro-1 HUT observation with an aperture of $9''.4\times116''$ (Ferguson et al. 1991), and its $(1550-V)$ comes from the IUE observations. As the far-UV light is more concentrated toward the centre of the galaxy than the optical light (Ohl et al. 1998), the value of $(1550-V)$ for NGC 1399 should be considered an upper limit for the galaxy area covered by the observation. The galaxies plotted are all elliptical galaxies except for NGC 5102, which is a S0 galaxy, and the nucleus of M 31, which is a Sb galaxy. Active galaxies or galaxies with large errors in $\beta_{\rm FUV}$ from BBBFL have not been plotted.

Overall, the model covers the observed range of properties reasonably well. Note in particular that the majority of galaxies lie in the part of the diagram where the UV contribution from binaries is expected to dominate (i.e. where $b_{\rm FUV}>0.5$). The location of M 60 and M 89 in this figure implies $f\sim0.01\%$ and $t_{\rm minor}\sim0.11\,$Gyr with $b_{\rm FUV}\sim0.5$. Interestingly, inspection of the HUT spectrum of M 60 (see the mid-left panel of figure 3 in Brown et al. (1997)) shows the presence of a marginal C IV absorption line near 1550Å. Chandra observations show that M 89 has a low luminosity AGN (Xu et al. 2005). This would make $(1550-V)$ bluer and may also provide indirect evidence for low levels of star formation.

The galaxy NGC 1399 requires special mention, as it is UV-bright and the young star-hypothesis was believed to have been ruled out due to the lack of strong C IV absorption lines in its HUT spectrum (Ferguson et al. 1991). However, any young star signature, if it exists, would have been diluted greatly in the HUT spectrum, as the aperture of the HUT observation is much larger than that of the IUE observation covering mainly the galaxy nucleus.

Our model is sensitive to both low levels and high levels of star formation. It suggests that elliptical galaxies had some star formation activity in the relatively recent past ($\sim1\,$Gyr ago). AGN and supernova activity may provide qualitative supporting evidence for this picture, since the former often appears to be accompanied

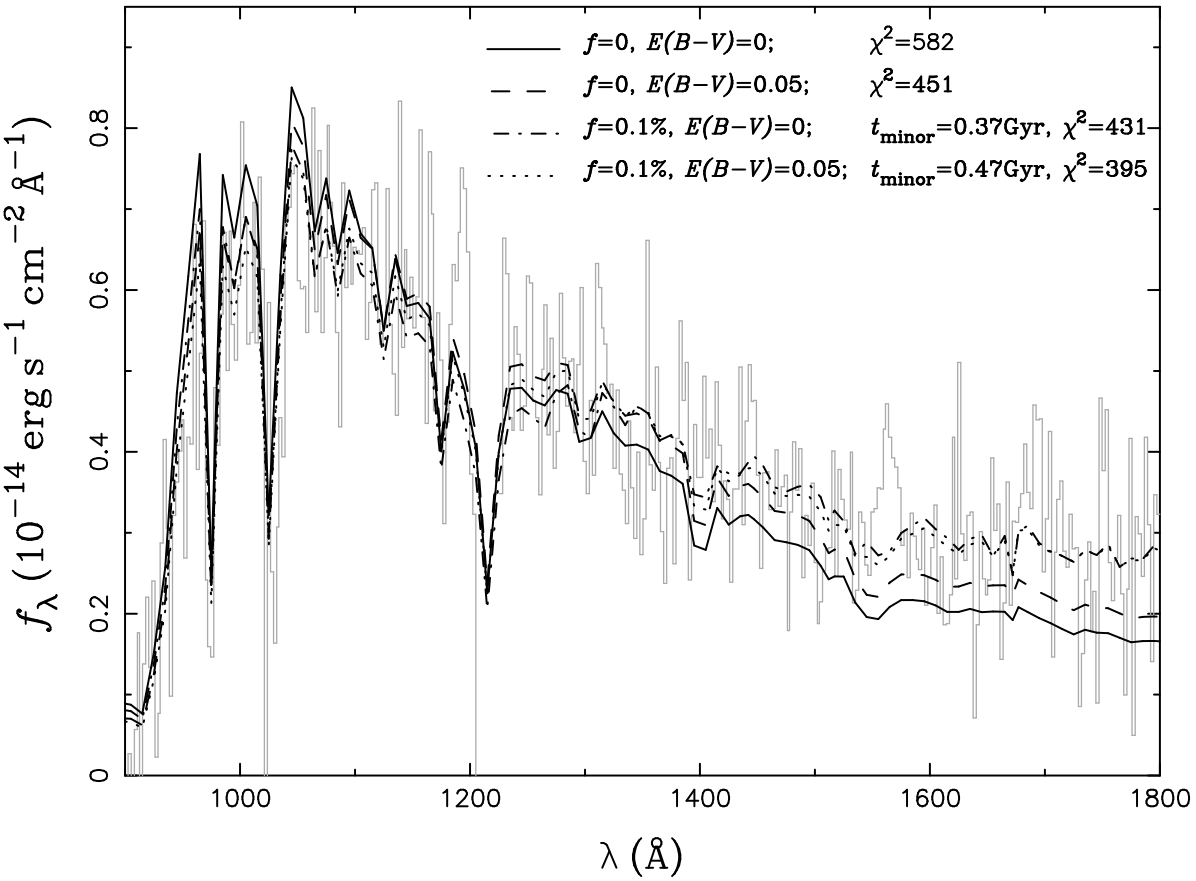

Figure 11. Far-UV SED fitting of NGC 3379, a standard elliptical galaxy. The grey histogram represents the HUT observations of Brown et al. (1997) with 337 bins, while the other curves are based on our theoretical model with different assumptions about a minor recent population and different amounts of extinction. The age of the old, dominant population, $t_{\rm major}$, is assumed to be 10 Gyr in all cases. The minor population, making up a total fraction f of the stellar mass of the galaxy, is assumed to have experienced a starburst $t_{\rm minor}$ ago, as indicated, lasting for 0.1 Gyr. To model the effects of dust extinction, we applied the internal dust extinction model of Calzetti et al. (2000). For a given f and $E(B-V)$, we varied the galaxy mass and the age of the minor population. For each case, the curves give the fits obtained. Note that the best fits require the presence of a minor young population.

by active star formation, while supernovae, both core collapse and thermonuclear, tend to occur mainly within 1 – 2 Gyr after a starburst in the most favoured supernova models. In Figure 12, we have plotted 13 early-type galaxies altogether. Using the Padova-Asiago supernova online catalogue[4], which lists supernovae recorded ever since 1885, we found 8 supernovae in six of the galaxies: SN 1885A (Type I) in M 31, SN 1969Q (type unavailable) in M 49, SN 2004W (Type Ia) in M 60, SN 1939B (Type I) in M 59, SN 1957B (Type Ia), SN 1980I (Type Ia), SN 1991bg (Type Ia) in M 84 and SN 1935B (type unavailable) in NGC 3115. The majority of supernovae in these galaxies appear to be of Type Ia.

4.3.3 Colour-colour diagrams

Similar to the above subsection, we have constructed composite stellar population models for elliptical galaxies consisting of a major old population ($t_{\rm major} = 10\,{\rm Gyr}$) and a minor younger population, but for colour-colour diagrams.

Figure 13 shows the appearance of a galaxy in the colour-colour diagrams of $(1550-V)$ versus $(1550-2500)$ (panel (a)) and $(2000-V)$ versus $(1550-2500)$ (panel (b)) in the CSP model for different fractions f and different ages of the minor population. Solid squares in panel (a) of the figure are for quiescent early-type galaxies observed with IUE by BBBFL and the data points are taken from table 2 of Dorman, O'Connell & Wood (1995). The observed data points are located in a region without recent star formation or with a very low level of recent star formation ($f \lesssim 0.1\%$). Therefore, the observations are naturally explained with our model. Panel (a) shows the epoch when the effects of the starburst fade away, leading to a fast evolution of the galaxy colours, and the diagram therefore provides a potentially powerful diagnostic to identify a minor starburst in an otherwise old elliptical galaxy that occurred up to ~ 2 Gyr ago. For larger ages, the curves tend to converge in the $(1550-2500)$ versus $(1550-V)$ diagram. Note that this is not so much the case in the $(1550-2500)$ versus $(2000-V)$ diagram, which therefore could provide better diagnostics.

Figure 14 is a diagram of $(B-V)$ versus $(2000-V)$ for a CSP with a major population age $t_{\rm major} = 10\,{\rm Gyr}$ and variable minor population age $t_{\rm minor}$ and various minor population mass fractions

[4] *http://web.pd.astro.it/supern/snean.txt*

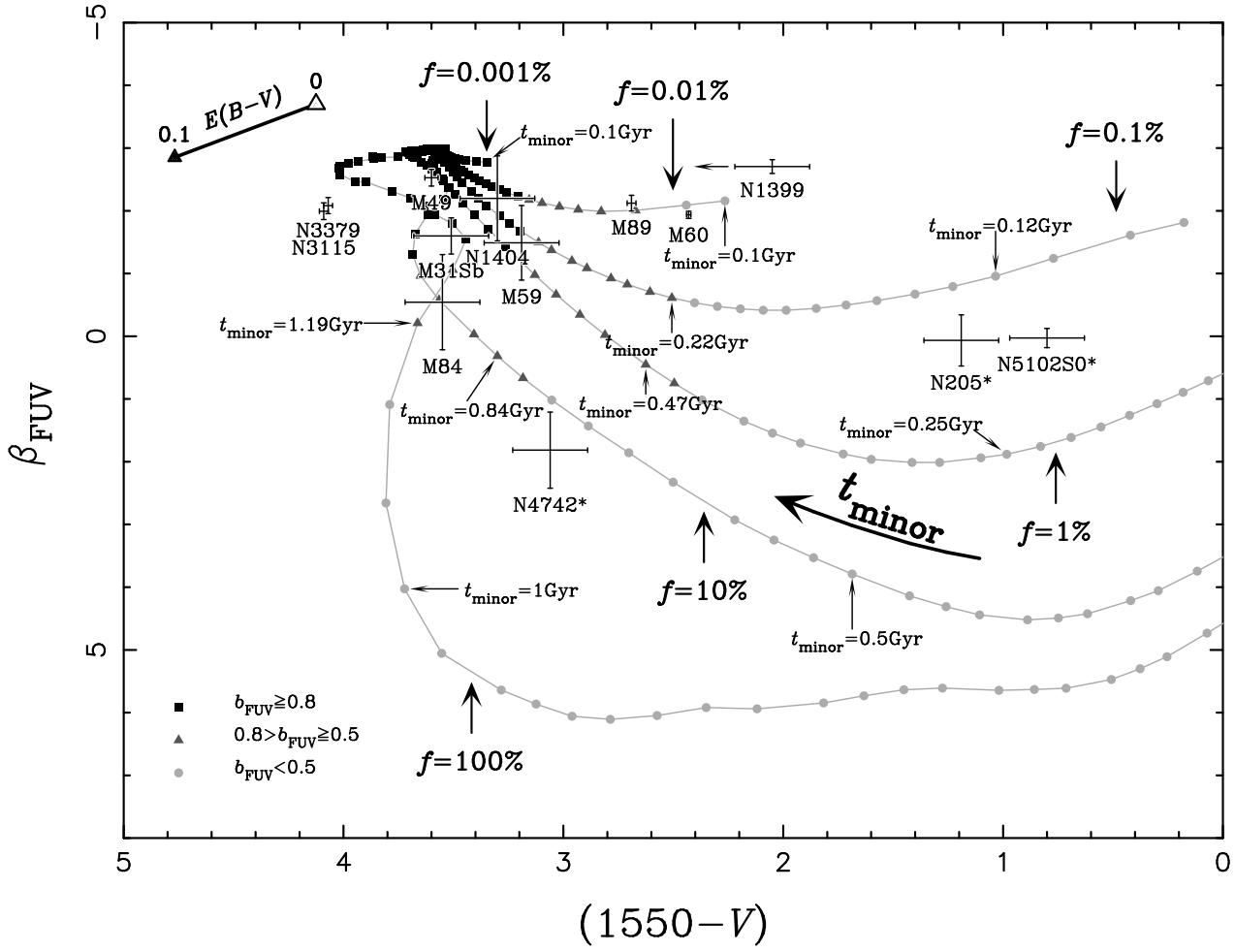

Figure 12. Evolution of far-UV properties [the slope of the far-UV spectrum, $\beta_{\rm FUV}$, versus $(1550-V)$] for a composite stellar population (CSP) model of elliptical galaxies with a major population age of $t_{\rm major}=10\,$Gyrs (Set 6). The mass fraction of the younger population is denoted as f and the time since the formation as $t_{\rm minor}$ [squares, triangles or dots are plotted in steps of $\Delta\log(t)=0.025$]. Note that the model for $f=100\%$ shows the evolution of a simple stellar population with age $t_{\rm minor}$. The legend is for $b_{\rm FUV}$, which is the fraction of the UV flux that originates from hot subdwarfs resulting from binary interactions. The effect of internal extinction is indicated in the top-left corner, based on the Calzetti internal extinction model with $E(B-V)=0.1$ (Calzetti et al. , 2000). For comparison, we also plot galaxies with error bars from HUT (Brown et al. , 1997) and IUE observations (BBBFL). The galaxies with strong signs of recent star formation are denoted with an asterisk (NGC 205, NGC 4742, NGC 5102).

f. Overlayed on this diagram is figure 2 of Deharveng, Boselli & Donas (2002) for observational data points of early-type galaxies. NGC 205 and NGC 5102 (the circles with crosses above the line $(2000-V)=1.4$) are known to have direct evidence of massive star formation (Hodge 1973; Pritchet 1979); therefore Deharveng, Boselli & Donas (2002) individually examined the seven galaxies with $(2000-V)<1.4$ in their sample for suspected star formation. CGCG 119053, CGCG 97125, VCC 1499 (the three solid squares with big stars) showed hints of star formation, NGC 4168 (the solid square with a big triangle) has a low-luminosity Seyfert nucleus and CGCG 119030 (the solid square with a big diamond) could be a spiral galaxy instead of an elliptical galaxy. However, no hint of star formation has been found for VCC 616 (the solid square on the far-left above the line $(2000-V)=1.4$) and CGCG 119086 (the solid square on the far-right above the line $(2000-V)=1.4$). Our model can explain the observations satisfactorily except for CGCG 119086, which needs further study.

Figure 15 shows the diagrams of $(FUV-r)_{\rm AB}$ versus $(FUV-NUV)_{\rm AB}$ for a CSP galaxy model with a major population age $t_{\rm major}=10\,$Gyr and variable minor population age $t_{\rm minor}$ and various minor population mass fractions f. In these diagrams, the colours are not shown in the restframe, but have been redshifted (i.e. the wavelength is $(1+z)$ times the restframe wavelength, where z is the redshift); panel (a) is for a redshift of $z=0.05$ and panel (b) for $z=0.15$. Overlayed on the two panels are quiescent early-type galaxies observed with GALEX by Rich et al. (2005). The observed galaxies are for a redshift range $0<z<0.1$ (panel (a)) and $0.1<z<0.2$ (panel (b)). We note that most of the quiescent galaxies are located in the region with $f\lesssim 1\%$.

In Figures 13 to 15, we adopted a major population age of $t_{\rm major}=10\,$Gyr, and the colours are intrinsic. However, adopting a different age for the major population can change the diagrams; for example, a larger age leads to bluer $(1550-2500)$ or $(FUV-NUV)$ colours. In contrast, internal dust extinction shifts the curves towards redder colours (Calzetti et al. 2000). Considering the uncertainties in the modelling, we take our model to be in reasonable agreement with the observations.

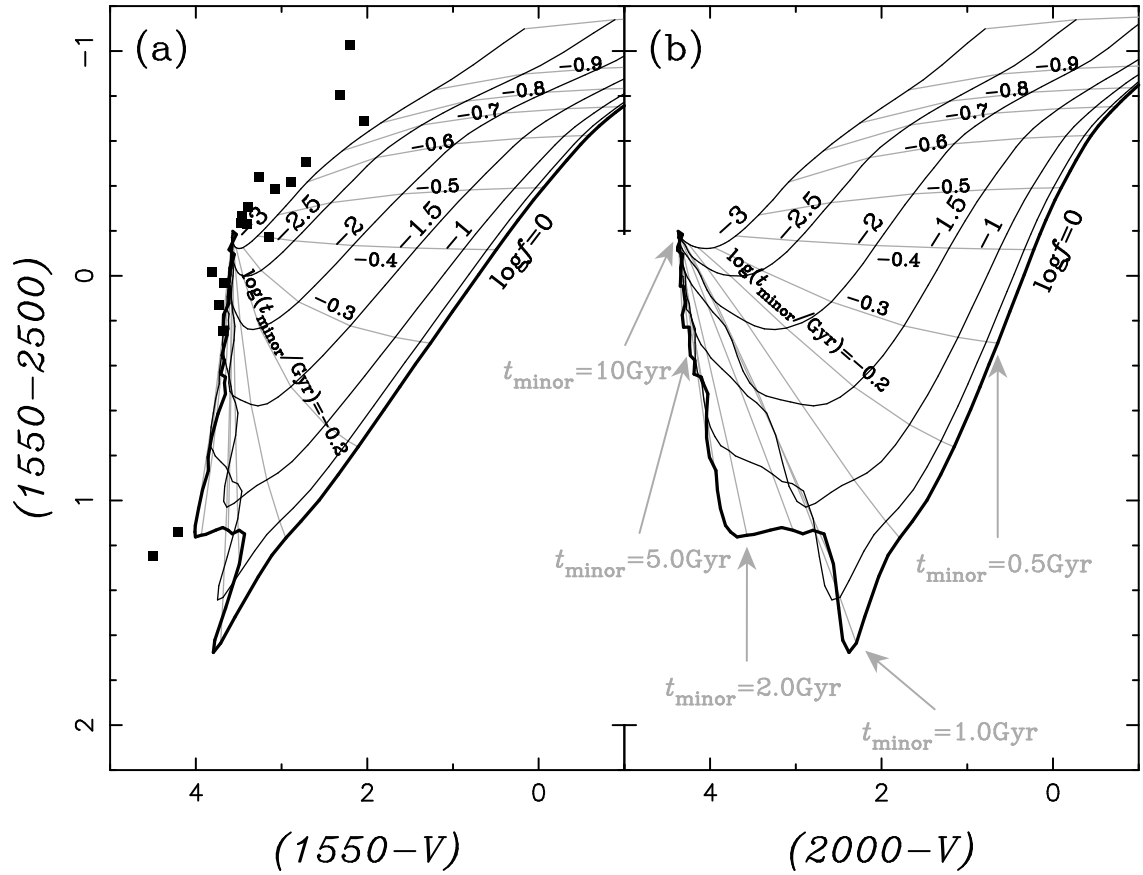

Figure 13. The diagrams of $(1550-V)$ versus $(1550-2500)$ (a) and $(2000-V)$ versus $(1550-2500)$ (b) for a composite stellar population (CSP) model of elliptical galaxies with a major population age of $t_{\rm major}=10\,{\rm Gyrs}$ (Set 6). Solid curves are for given minor population fractions f and are plotted, from left to right, in steps of $\Delta\log(f)=0.5$, as indicated. Light grey curves are for fixed minor population ages $t_{\rm minor}$ and are plotted, from top to bottom, in steps of $\Delta\log(t_{\rm minor}/{\rm Gyr})=0.1$, as indicated. Note that the colours are given in the restframe and intrinsic. The thick solid curve for $f=100\%$ actually shows the evolution of a simple stellar population with age $t_{\rm minor}$. Solid squares are for quiescent early-type galaxies observed with IUE by BBBFL and the data points are taken from Dorman, O'Connell & Wood (1995).

4.3.4 UV-upturn magnitudes and their evolution with redshift

There is an observed spread in the $(1550-V)$, $(1550-2500)$ and $(2000-V)$ colours of early-type galaxies. As can be seen from Figures 12, 13, and 14, this spread is satisfactorily explained by our model.

Brown et al. (2003) showed with HST observations that the UV-upturn does not evolve much with redshift, a result apparently confirmed by Rich et al. (2005) with GALEX observation of a large sample. This is contrary to the prediction of both the metal-poor and the metal-rich model, as both models require a large age for the hot subdwarfs and therefore predict that the UV-upturn should decline rapidly with redshift. Our binary model, however, predicts that that UV-upturn does not evolve much with redshift (see Figures 3 and 4), consistent with the recent observations.

Lee et al. (2005) and Ree et al. (2007) studied the look-back time evolution of the UV-upturn from the brightest elliptical galaxies in 12 clusters at redshift $z<0.2$ with GALEX. Compared to local giant elliptical galaxies, they found that the UV-upturn of the 12 galaxies is redder. However, the local giant elliptical galaxies are quite special. NGC 1399 and M 87, with the strongest UV-upturn, have the largest known specific frequencies of globular clusters (Ostrov, Geisler & Forte 1993), and M 87 hosts an active galactic nuclei (AGN) with the best-known jet (Curtis 1918; Waters & Zepf 2005). Given a larger sample of elliptical galaxies, no matter how luminous they are, and a bigger redshift range, the UV-upturn is not found to decline with redshift.

4.3.5 Implication for star formation history of early-type galaxies

Boselli et al. (2005) studied the UV properties of 264 early-type galaxies in the Virgo cluster with GALEX. They showed that $(FUV-NUV)_{\rm AB}$ ranges from 3 to 0, consistent with the theoretical range shown in panel (b) of Figure 4. The colour index $(FUV-NUV)_{\rm AB}$ of those galaxies becomes bluer with luminosity from dwarfs ($L_{\rm H}\sim10^8L_{\rm H,\odot}$) to giants ($L_{\rm H}\sim10^{11.5}L_{\rm H,\odot}$), i.e. a luminous galaxy tends to have a bluer $(FUV-NUV)_{\rm AB}$. Panel (b) of Figure 4 shows that $(FUV-NUV)_{\rm AB}$ becomes bluer with population age for $t_{\rm SSP}>1\,{\rm Gyr}$. Taking the stellar populations as an "averaged" SSP, we may conclude that a luminous

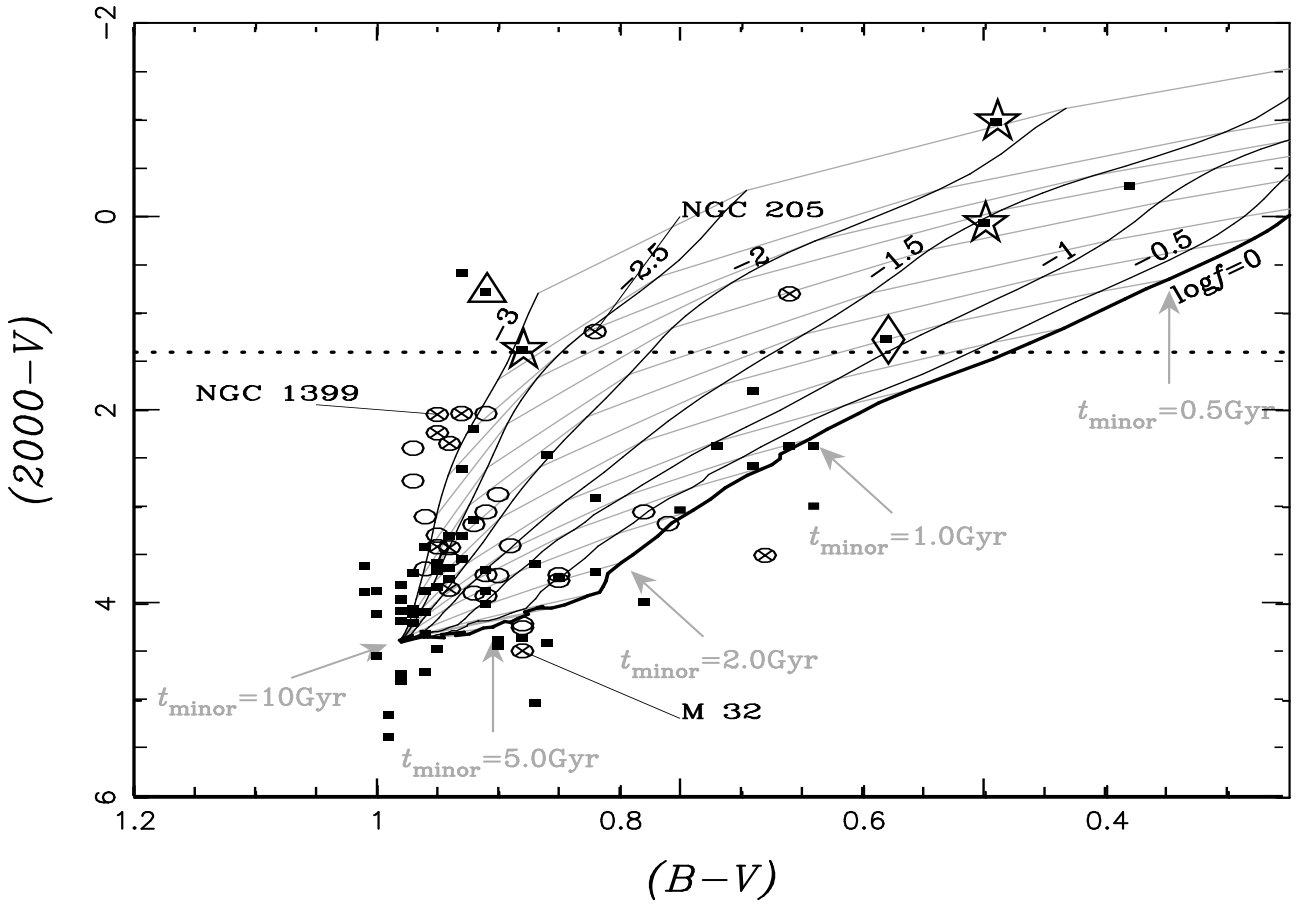

Figure 14. The diagrams of $(B-V)$ versus $(2000-V)$ for a composite stellar population (CSP) model of elliptical galaxies with a major population age of $t_{\rm major}=10\,{\rm Gyrs}$ (Set 6). Solid curves are for given minor population fractions f and are plotted, from left to right, in steps of $\Delta\log(f)=0.5$, as indicated. Light grey curves are for fixed minor population ages $t_{\rm minor}$ and are plotted, from top to bottom, in steps of $\Delta\log(t_{\rm minor}/{\rm Gyr})=0.1$, as indicated. The thick solid curve for $f=100\%$ actually shows the evolution of a simple stellar population with age $t_{\rm minor}$. Note that the colours are intrinsic and are plotted in the restframe. Overlayed on this diagram is figure 2 of Deharveng, Boselli & Donas (2002), in which solid squares are for their sample observed with the FOCA experiment and open circles (including circles with crosses) are for the sample of BBBFL observed with IUE. Crosses denote objects that have been studied in detail with HUT or HST. For galaxies bluer than $(2000-V)=1.4$, solid squares with big stars and circles with crosses are for galaxies with recent star formation. NGC 4168 (solid square with a big triangle) has a low-luminosity Seyfert nucleus. CGCG 119030 (solid square with a big diamond) could be misclassified as an elliptical, as it is classified as a spiral in the NASA/IPAC Extragalactic Database (NED).

early-type galaxy is older, or in other words, the less luminous an early-type galaxy is, the younger the stellar population is or the later the population formed.

4.4 The UV-upturn and metallicity

As far as we know, metallicity does not play a significant role in the mass-transfer process or the envelope ejection process for the formation of hot subdwarfs, although it may affect the properties of the binary population in more subtle ways. We therefore expect that $(FUV-r)_{\rm AB}$ or $(1550-V)$ from our model is not very sensitive to the metallicity of the population, This is in agreement with the recent large sample of GALEX observations by Rich et al. (2005). Boselli et al. (2005) and Donas et al. (2006) studied nearby early-type galaxies with GALEX. Neither of them show that $(FUV-r)_{\rm AB}$ correlates significantly with metallicity, However, both of them found a positive correlation between $(FUV-NUV)_{\rm AB}$ and metallicity. This can possibly be explained with our model. The UV-upturn magnitudes $(FUV-r)_{\rm AB}$ or $(1550-V)$ does not evolve much with age for $t_{\rm SSP}>1\,{\rm Gyr}$ while $(FUV-NUV)_{\rm AB}$ decreases significantly with age (see Figures 3 and 4). A galaxy of high metallicity may have a larger age and therefore a stronger $(FUV-NUV)_{\rm AB}$.

4.5 Comparison with previous models

Both metal-poor and metal-rich models are quite *ad hoc* and require a large age for the hot subdwarf population (Section 1), which implies that the UV-upturn declines rapidly with look-back time or redshift. In our model, hot subdwarfs are produced naturally by envelope loss through binary interactions, which do not depend much on the age of the population older than $\sim 1\,{\rm Gyr}$, and therefore our model predicts little if any evolution of the UV-upturn with redshift. Note, however, that $(FUV-NUV)_{\rm AB}$ declines significantly more with redshift than $(FUV-r)_{\rm AB}$, as the contribution to the near-UV from blue stragglers resulting from binary interactions becomes less important for an older population.

The metal-rich model predicts a positive correlation between the magnitude of the UV-upturn and metallicity; for example, $(1550-V)$ correlates with metallicity. However, such a correla-

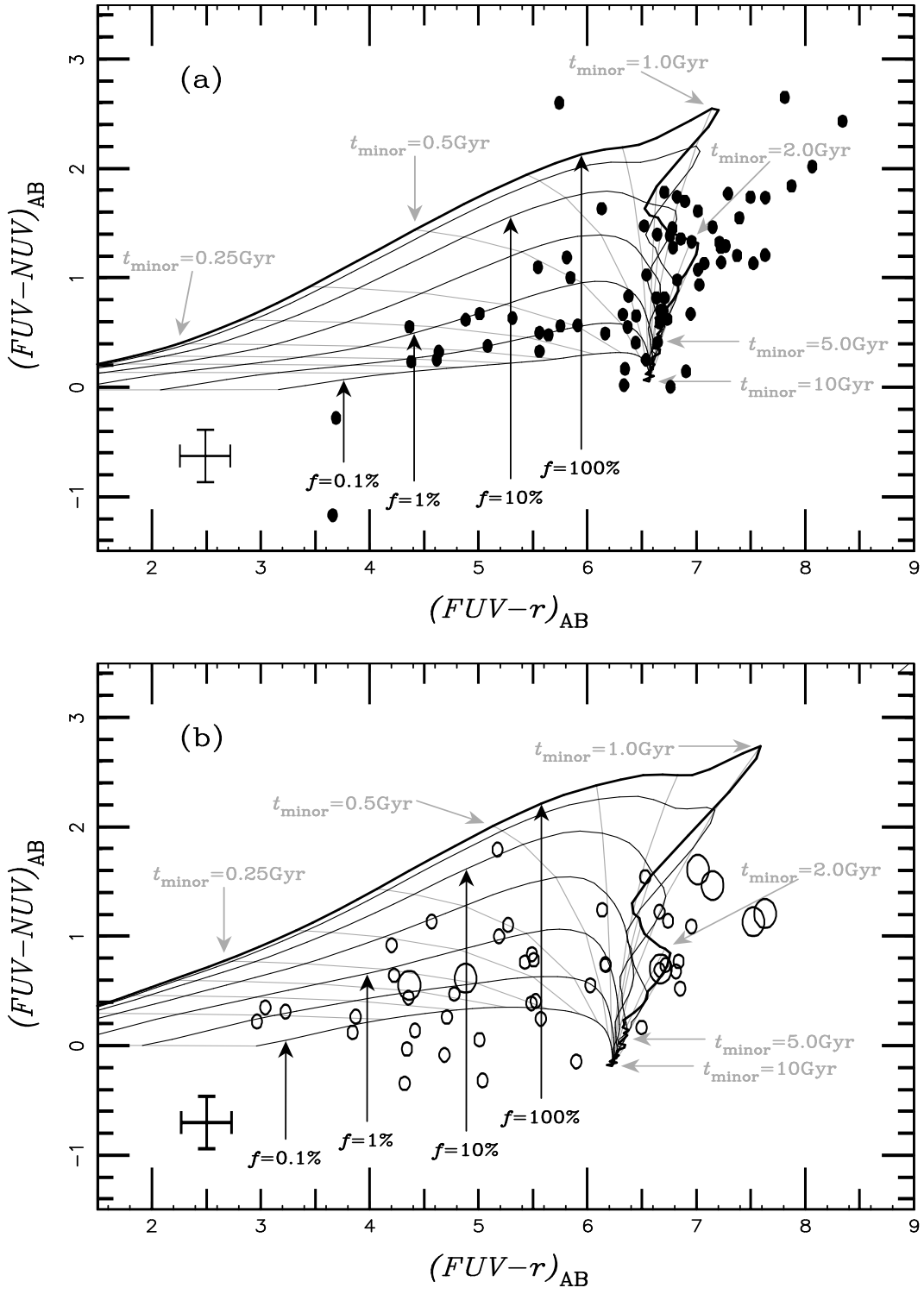

Figure 15. The diagrams of $(FUV-r)_{\rm AB}$ versus $(FUV-NUV)_{\rm AB}$ for a composite stellar population (CSP) with a major population age of $t_{\rm major}=10\,{\rm Gyrs}$ (Set 6). Solid curves are for given minor population fractions f and are plotted, from bottom to top, in steps of $\Delta\log(f)=0.5$, as indicated. Light grey curves are for fixed minor population ages $t_{\rm minor}$ and are plotted, from left to right, in steps of $\Delta\log(t_{\rm minor}/{\rm Gyr})=0.1$, as indicated. The thick solid curve for $f=100\%$ actually shows the evolution of a simple stellar population with age $t_{\rm minor}$. Note that the colours are intrinsic but not in the restframe. Panel (a) assumes a redshift of $z=0.05$ and panel (b) $z=0.15$. Overlayed on this diagram is figure 3 of Rich et al. (2005), in which circles are for their sample observed with GALEX for quiescent early-type galaxies. Filled circles (panel (a)) are observational data points for galaxies of $0<z<0.1$ and open circles (panel (b)) for $0.1<z<0.2$.

tion is not expected from our binary model as metallicity does not play an essential role in the binary interactions. Furthermore, even though the metal-rich model could in principle account for the UV-upturn in old, metal-rich giant ellipticals, it cannot produce a UV-upturn in lower-metallicity dwarf ellipticals. In contrast, in a binary model, the UV-upturn is universal and can account for UV-upturns from dwarf ellipticals to giant ellipticals.

5 SUMMARY AND CONCLUSION

By applying the binary scenario of Han et al. (2002; 2003) for the formation of hot subdwarfs, we have developed an evolutionary population synthesis model for the UV-upturn of elliptical galaxies based on a first-principle approach. The model is still quite simple and does not take into account more complex star-formation histories, possible contributions to the UV from AGN activity, non-solar metallicity or a range of metallicities. Moreover, the binary population synthesis is sensitive to uncertainties in the binary modelling itself, in particular the mass-ratio distribution and the condition for stable and unstable mass transfer (Han et al. 2003). We have varied these parameters and found these uncertainties do not change the qualitative picture, but affect some of the quantitative estimates.

Despite its simplicity, our model can successfully reproduce most of the properties of elliptical galaxies with a UV excess: the range of observed UV excesses, both in $(1550-V)$ and $(2000-V)$ (e.g. Deharveng, Boselli & Donas, 2002), and their evolution with redshift. The model predicts that the UV excess is not a strong function of age, and hence is not a good indicator for the age of the dominant old population, as has been argued previously (Yi et al. 1999), but is very consistent with recent GALEX findings (Rich et al. 2005). We typically find that the $(1550-V)$ colour changes rapidly over the first 1 Gyr and only varies slowly thereafter. This also implies that all old galaxies should show a UV excess at some level. Moreover, we expect that the model is not very sensitive to the metallicity of the population. The UV-upturn is therefore expected to be universal.

Our model is sensitive to both low levels and high levels of star formation. It suggests that elliptical galaxies had some star formation activity in the relatively recent past ($\sim$ 1 Gyr ago). AGN and supernova activity may provide supporting evidence for this picture.

The modelling of the UV excess presented in this study is only a starting point: with refinements in the spectral modelling, including metallicity effects, and more detailed modelling of the global evolution of the stellar population in elliptical galaxies, we propose that this becomes a powerful new tool helping to unravel the complex histories of elliptical galaxies that a long time ago looked so simple and straightforward.

ACKNOWLEDGEMENTS

We are grateful to an anonymous referee for valuable comments which help to improve the presentation, to Kevin Schawinski for numerous discussions and suggestions, to Thorsten Lisker for insightful comments leading to Section 4.3.5. This work was in part supported by the Natural Science Foundation of China under Grant Nos. 10433030 and 10521001, the Chinese Academy of Sciences under Grant No. KJCX2-SW-T06 (Z.H.), and a Royal Society UK-China Joint Project Grant (Ph.P and Z.H.).

REFERENCES

Allard F., Wesemael F., Fontaine G., Bergeron P., Lamontagne R., 1994, AJ, 107, 1565
Anders E., Grevesse N., 1989, Geochimica et Cosmochimica Acta, 53, 197
Aznar Cuadrado R., Jeffery C.S., 2001, A&A, 368, 994
Boselli A. et al. , 2005, ApJ, 629, L29
Brassard P., Fontaine G., Billéres M., Charpinet S., Liebert J., Saffer R.A., 2001, ApJ, 305, 228
Bressan A., Chiosi C., Fagotto F., 1994, ApJS, 94, 63
Bressan A., Chiosi C., Tantalo R., 1996, A&A, 311, 425
Brown T.M., 2004, Ap&SS, 291, 215
Brown T.M., Ferguson H.C., Davidsen A.F., 1995, ApJ, 454, L15
Brown T.M., Ferguson H.C., Davidsen A.F., Dorman B., 1997, ApJ, 482, 685
Brown T.M., Ferguson H.C., Deharveng J.M., Jedrzejewski R.I., 1998, ApJ, 508, L139
Brown T.M., Bowers C.W., Kimble R.A., Ferguson H.C., 2000a, ApJ, 529, L89
Brown T.M., Bowers C.W., Kimble R.A., Sweigart A.V., 2000b, ApJ, 532, 308
Brown T.M., Ferguson H.C., Smith E., Bowers C.B., Kimble R., Renzini A., Rich R.M., 2003, ApJ, 584, L69
Bruzual A.G., Charlot S., 1993, ApJ, 405, 538
Bruzual A.G., Charlot S., 2003, MNRAS, 344, 1000
Burstein D., Bertola F., Buson L.M., Faber S.M., Lauer T.R., 1988, ApJ, 328, 440 (BBBFL)
Calzetti D., Bohlin R.C., Kinney A.L., Koornneef J., Storchi-Bergmann T., 2000, ApJ, 533, 682
Carraro G., Girardi L., Bressan A., Chiosi C., 1996, A&A, 305, 849
Carroll M., Press W.H., Turner E.L., 1992, ARA&A, 30, 499
Charpinet S., Fontaine G., Brassard P., Billères M., Green E.M., Chayer P., 2005, A&A, 443, 251
Chen X., Han Z., 2004, MNRAS, 355, 1182
Chiosi C., Vallenari A., Bressan A., 1997, A&AS, 121, 301
Code A.D., 1969, PASP, 81, 475
Curtis H.D., 1918, Publ. Lick Obs., 13, 31
D'Cruz N.L., Dorman B., Rood R.T., O'Connell R.W., 1996, ApJ, 466, 359
Deharveng J.-M., Boselli A., Donas J., 2002, A&A, 393, 843
Dewi J., Tauris T., 2000, A&A, 360, 1043
Donas J., Milliard B., Laget M., Buat V., 1990, A&A, 235, 60
Donas J., Milliard B., Laget M., 1995, A&A, 303, 661
Donas J. et al. , 2006, astro-ph/0608594
Dorman B., Rood R.T., O'Connell R.W., 1993, ApJ, 419, 596
Dorman B., O'Connell R.W., Rood R.T., 1995, ApJ, 442, 105
Downes R.A., 1986, ApJS, 61, 569
Eggleton P.P., 1971, MNRAS, 151, 351
Eggleton P.P., 1972, MNRAS, 156, 361
Eggleton P.P., 1973, MNRAS, 163, 179
Eggleton P.P., Fitchett M.J., Tout C.A., 1989, ApJ, 347, 998
Eggleton P.P., Tout C.A., 1989, in Batten A.H., ed., Algols, Kluwer, Dordrecht, p. 164
Fukugita M., Ichikawa T., Gunn J.E., Doi M., Shimasaku K., Schneider D.P., 1996, AJ, 111, 1748
Ferguson D.H., Green R.F., Liebert J., 1984, ApJ, 287, 320
Ferguson, H.C. et al. , 1991, ApJ, 382, L69
Goldberg D., Mazeh T., 1994, A&A, 282, 801
Green R.F., Schmidt M., Liebert J., 1986, ApJS, 61, 305
Gregg M.D., Ferguson H.C., Minniti D., Tanvir N., Catchpole R., 2004, AJ, 127, 1441
Greggio L., Renzini A., 1990, ApJ, 364, 35
Gunn J.E., Stryker L.L., Tinsley B.M., 1981, ApJ, 249, 48
Gunn J.E. et al. , 1998, AJ, 116, 3040
Halbwachs J.L., Mayor M., Udry S., 1998, in Rebolo R., Martin E.L., Zapatero Osorio M.R., eds, Brown Dwarfs and Extrasolar Planets, ASP Conf. Ser., Vol. 134, p. 308
Han Z., 1995, Ph.D. Thesis (Cambridge)
Han Z., 1998, MNRAS, 296, 1019

Han Z., Podsiadlowski Ph., 2004, MNRAS, 350, 1301
Han Z., Webbink R.F., 1999, A&A, 349, L17
Han Z., Podsiadlowski Ph., Eggleton P.P., 1994, MNRAS, 270, 121
Han Z., Podsiadlowski Ph., Eggleton P.P., 1995, MNRAS, 272, 800
Han Z., Eggleton P.P., Podsiadlowski Ph., Tout C.A., 1995, MNRAS, 277, 1443
Han Z., Tout C.A., Eggleton P.P., 2000, MNRAS, 319, 215
Han Z., Eggleton P.P., Podsiadlowski Ph., Tout C.A., Webbink R.F., 2001, in Podsiadlowski Ph., Rappaport S., King A.R., D'Antona F., Burderi L., eds, Evolution of Binary and Multiple Star Systems, ASP Conf. Ser., Vol. 229, p. 205
Han Z., Podsiadlowski Ph., Maxted P.F.L., Marsh T.R., Ivanova N., 2002, MNRAS, 336, 449
Han Z., Podsiadlowski Ph., Maxted P.F.L., Marsh T.R., 2003, MNRAS, 341, 669 (HPMM)
Heacox W.D., 1995, AJ, 109, 2670
Heber U., 1986, A&A, 155, 33
Heber U., Moehler S., Napiwotzki R., Thejll P., Green E.M., 2002, A&A, 383, 938
Heber U. et al. , 2004, A&A, 420, 251
Hills J.G., 1971, A&A, 12, 1
Hjellming M.S., Webbink R.F., 1987, ApJ, 318, 794
Hodge P.W., 1973, ApJ, 182, 671
Hurley J.R., Tout C.A., Pols, O.R., 2002, MNRAS, 329, 897
Hurley J.R., Pols O.R., Aarseth S.J., Tout C.A., 2005, MNRAS, 363, 293
Iben I. Jr., Renzini A., 1983, ARA&A, 21, 271
Iben I. Jr., Tutukov A.V., 1986, ApJ, 311, 753
Jeffery C.S., Pollacco D.L., 1998, MNRAS, 298, 179
Johnson H.L., Morgan W.W., 1953, ApJ, 117, 313
Kaviraj S., et al. 2006, ApJ, in press (available at http://xxx.lanl.gov/abs/astro-ph/0601029)
Kilkenny D., Koen C., Jeffery J., Hill C.S., O'Donoghue D., 1999, MNRAS, 310, 1119
Kjærgaard P., 1987, A&A, 176, 210
Koen C., Orosz J.A., Wade R.A., 1998, MNRAS, 300, 695
Kroupa P., Tout C.A., Gilmore G., 1993, MNRAS, 262, 545
Kurucz R.L., 1992, in Barbuy B., Renzini A., eds, Proc. IAU Symp. 149, The Stellar Population of Galaxies, Kluwer, Dordrecht, p.225
Lee Y.W., 1994, ApJ, 430, L113
Lee Y.W. et al. , 2005, ApJ, 619, L103
Lejeune T., Cuisinier F., Buser R., 1997, A&AS, 125, 229
Lejeune T., Cuisinier F., Buser R., 1998, A&AS, 130, 65
Lisker T., Heber U., Napiwotzki R., Christlieb N., Reimers D., Homeier D., 2004, Ap&SS, 291, 351
Lisker T., Heber U., Napiwotzki R., Christlieb N., Han Z., Homeier D., Reimers D., 2005, A&A, 430, 223
Martin D.C. et al. , 2005, ApJ, 619, L1
Maxted P.F.L., Moran C.K.J., Marsh T.R., Gatti A.A., 2000, MNRAS, 311, 877
Maxted P.R.L., Marsh T.R., North R.C., 2000, MNRAS, 317, L41
Maxted P.F.L., Heber U., Marsh T.R., North R.C., 2001, MNRAS, 326, 1391
Mazeh T., Goldberg D., Duquennoy A., Mayor M., 1992, ApJ, 401, 265
Mengel J.G., Norris J., Gross P.G., 1976, ApJ, 204, 488
Miller G.E., Scalo J.M., 1979, ApJS, 41, 513
Morales-Rueda L.,Maxted P.F.L., Marsh T.R., 2004, Ap&SS, 291, 299
Morales-Rueda L.,Maxted P.F.L., Marsh T.R., Kilkenny D., O'Donoghue D., 2006, Baltic Astronomy, 15, 187
Moran C., Maxted P., Marsh T.R., Saffer R.A., Livio M., 1999, MNRAS, 304, 535
Mochkovitch R., 1986, A&A, 157, 311
Napiwotzki R., Edelmann H., Heber U., Karl C., Drechsel H., Pauli E.-M., Christlieb N., 2001, A&A, 378, L17
Nesci R., Perola G.C., 1985, A&A, 145, 296
Ohl R.G. et al. , 1998, ApJ, 505, L11
O'Connell R.W., 1999, ARA&A, 37, 603
Oke J.B., Gunn J.E., 1983, ApJ, 266, 713
Orosz J.A., Wade R.A., 1999, MNRAS, 310, 773
Ostrov P., Geisler D., Forte J.C., 1993, AJ, 105, 1762
Paczyński B., 1965, Acta Astron., 15, 89
Paczyński B., 1976, in Eggleton P.P., Mitton S., Whelan J., eds, Structure and Evolution of Close Binaries, Kluwer, Dordrecht, p. 75
Paczyński B., Ziółkowski J., Żytkow A., 1969, in Hack M. ed., Mass Loss from Stars, Reidel, Dordrecht, P. 237
Plavec M., Ulrich R.K., Polidan R.S., 1973, PASP, 85, 769
Podsiadlowski Ph., Joss P.C, Hsu J.J.L., 1992, ApJ, 391, 246
Podsiadlowski, Ph., Rappaport, S., Pfahl, E., 2002, ApJ, 565, 1107
Pols O.R., Marinus M., 1994, A&A, 288, 475
Pols O.R., Tout C.A., Eggleton P.P., Han Z., 1995, MNRAS, 274, 964
Pols O.R., Schröder K.-P., Hurley J.R., Tout C.A., Eggleton P.P., 1998, MNRAS, 298, 525
Park J.H., Lee Y.W., 1997, ApJ, 476, 28
Pritchet C., 1979, ApJ, 231, 354
Rappaport S., Verbunt F., Joss P.C., 1983, ApJ, 275, 713
Ree C.H. et al. , 2007, ApJS, in press (available at http://xxx.lanl.gov/abs/astro-ph/0703503)
Reed M.D., Stiening R., 2004, PASP, 116, 506
Reimers D., 1975, Mem. R. Soc. Liège, 6ième Serie, 8, 369
Renzini A., 1981, in Effects of Mass Loss on Stellar Evolution, ed. C. Chiosi & R. Stalio (Dordrecht: Reidel), 319
Rich R.M. et al. , 2005, ApJ, 619, L107
Saffer R.A., Livio M., Yungelson L.R., 1998, ApJ, 502, 394
Saffer R.A., Bergeron P., Koester D., Liebert J., 1994, ApJ, 432, 351
Sandage A.R., 1953, AJ, 58, 61
Salim, S. et al. , 2005, ApJ, 619, L39
Schawinski K., et al. 2006, ApJ, in press (available at http://xxx.lanl.gov/abs/astro-ph/0601036)
Shatsky N., Tokovinin A., 2002, A&A, 382, 92
Smith J.A. et al. , 2002, AJ, 123, 2121
Soberman G.E., Phinney E.S., van den Heuvel E.P.J., 1997, A&A, 327, 620
Sweigart A.V., 1997, ApJ, 474, L23
Tantalo R., Chiosi C., Bressan A., Fagotto F., 1996, A&A, 311, 361
Terlevich A.I., Forbes D.A., 2002, MNRAS, 330, 547
Thomas D., Maraston C., Bender R., Mendes de Oliveira C., 2005, ApJ, 673, 694
Thejll P., Ulla A., MacDonald J., 1995, A&A, 303, 773
Tinsley B.M., 1968, ApJ, 151, 547
Tout C.A., Eggleton P.P., 1988, MNRAS, 231, 823
Tutukov A.V., Yungelson L.R., 1990, A.Zh., 67, 109
Ulla A., Thejll P., 1998, A&AS, 132, 1
Van Dyk S.D., Li W., Filippenko A.V., 2003, PASP, 115, 1
Verbunt F., Zwaan C., 1981, A&A, 100, L7
Waters C.Z., Zepf S.E., 2005, ApJ, 624, 656
Webbink R.F., 1984, ApJ, 277, 355
Webbink R. F., 1988, in Mikołajewska J., Friedjung M., Kenyon S. J., Viotti R., eds, The Symbiotic Phenomenon. Kluwer, Dordrecht, p. 311
Williams T., McGraw J.T., Mason P.A., Grashuis R., 2001, PASP, 113, 944
Wood J.H., Saffer R., 1999, MNRAS, 305, 820
Worthey G., 1994, ApJ, 95, 107
Xu Y., Xu H., Zhang Z., Kundu A., Wang Y., Wu. Y., 2005, ApJ, 631, 809
Yi S.K., 2004, Ap&SS, 291, 205
Yi S.K., Afshari E., Demarque P., Oemler Jr. A., 1995, ApJ, 453, L69
Yi S.K., Demarque P., Kim Y.C., 1997, ApJ, 482, 677
Yi S.K., Demarque P., Oemler Jr. A., 1997, ApJ, 486, 201
Yi S.K., Demarque P., Oemler Jr. A., 1998, ApJ, 492, 480
Yi S.K., Lee Y., Woo J., Park J., Demarque P., Oemler Jr. A., 1999, ApJ, 513, 128
Yi, S.K. et al. , 2005, ApJ, 619, L111
Zhang F., Li L., 2006, MNRAS, 370, 1181
Zhang F., Han Z., Li L., Hurley J.R., 2002, MNRAS, 334, 883
Zhang F., Han Z., Li L., Hurley J.R., 2004a, MNRAS, 350, 710
Zhang F., Han Z., Li L., Hurley J.R., 2004b, A&A, 415, 117
Zhang F., Han Z., Li L., Hurley J.R., 2005a, MNRAS, 357, 1088
Zhang F., Li L., Han Z., 2005b, MNRAS, 364, 503
Zhou X., Véron-Cetty M.P., Véron P., 1992, Acta Astrophysica Sinica, 12, 308

Zoccali M., Cassisi S., Frogel J.A., Gould A., Ortolani S., Renzini A., Rich R.M., Stephens A.W., 2000, ApJ, 530, 418